



Title	Controls on chemical evolution and rare element enrichment in crystallising albite-spodumene pegmatite and wallrocks: Constraints from mineral chemistry
Authors(s)	Barros, Renata, Kaeter, David, Menuge, Julian, Škoda, Radek
Publication date	2020-01
Publication information	Barros, Renata, David Kaeter, Julian Menuge, and Radek Škoda. "Controls on Chemical Evolution and Rare Element Enrichment in Crystallising Albite-Spodumene Pegmatite and Wallrocks: Constraints from Mineral Chemistry." Elsevier, January 2020. https://doi.org/10.1016/j.lithos.2019.105289 .
Publisher	Elsevier
Item record/more information	http://hdl.handle.net/10197/11555
Publisher's statement	This is the author's version of a work that was accepted for publication in Lithos. Changes resulting from the publishing process, such as peer review, editing, corrections, structural formatting, and other quality control mechanisms may not be reflected in this document. Changes may have been made to this work since it was submitted for publication. A definitive version was subsequently published in Lithos (VOL#, ISSUE#, (2019)) https://doi.org/10.1016/j.lithos.2019.105289
Publisher's version (DOI)	10.1016/j.lithos.2019.105289

Downloaded 2025-12-04 22:52:04

The UCD community has made this article openly available. Please share how this access benefits you. Your story matters! (@ucd_oa)



© Some rights reserved. For more information

Controls on chemical evolution and rare element enrichment in crystallising albite-spodumene pegmatite and wallrocks: constraints from mineral chemistry

Renata Barros^a, David Kaeter^{a,b}, Julian F. Menuge^{a,b} and Radek Škoda^c

^aSchool of Earth Sciences, University College Dublin, Belfield, Dublin 4, Ireland

(corresponding author, email: renataferbar@gmail.com)

^biCRAG, University College Dublin, Belfield, Dublin 4, Ireland

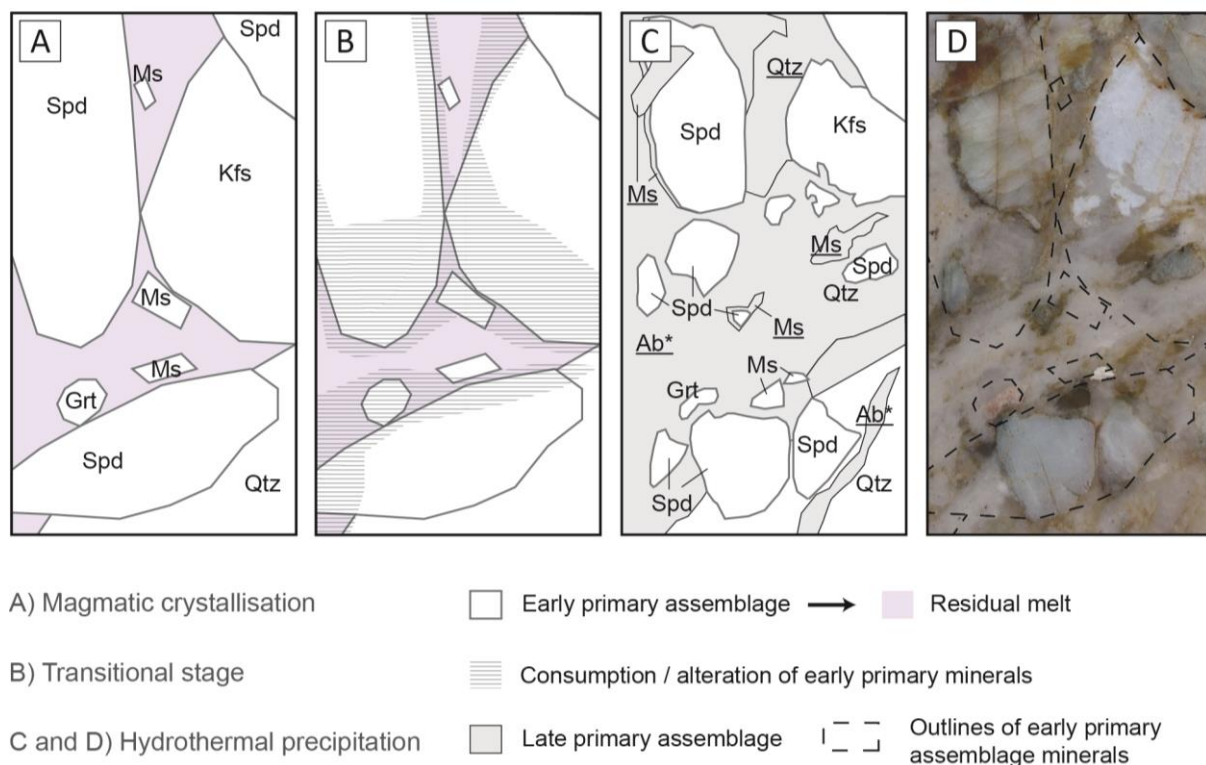
^cDepartment of Geological Sciences, Masaryk University, Kotlářská 267/2, 611 37 Brno, Czech Republic

Abstract

Internal differentiation and consequent geochemical evolution in pegmatites are significant processes in the development of economically viable deposits of metal-bearing minerals. Albite-spodumene pegmatites, which represent important resources of Li and Ta worldwide, challenge the general rules of pegmatite petrogenesis as these are nearly homogeneous bodies with little or no intrusion-scale pegmatite zonation. Bulk intrusion concentrations of Li are in the uppermost range obtained by magmatic enrichment experiments, around 2 wt. % Li₂O, and extensive volumes of saccharoidal or platy albite are present. In Leinster, southeast Ireland, weakly zoned to homogeneous albitised spodumene pegmatites and their wallrocks were studied to compare mineral chemistry variations and understand the internal evolution of pegmatites, characteristics linked to the poor development of zonation, and links between internal evolution and pegmatite-wallrock interactions. Leinster pegmatites present mineralogical, textural and geochemical characteristics coherent with Li-saturation, and possibly supersaturation, prior to crystallisation. Weak border to centre zonation in the thickest bodies can be attributed to geochemically evolved initial melt, likely leading to nearly

contemporaneous crystallisation throughout the intrusion and resulting in limited internal geochemical fractionation. Increased abundance of minerals bearing highly incompatible elements (e.g. columbite-group minerals and cassiterite) and network modifiers (e.g. phosphates) in albitite indicates it is a fractionation product from pegmatite crystallisation. Enrichment in incompatible elements B, Li, Rb, Cs and F in spodumene pegmatite exocontacts in different country rock types suggests unmixing of a hydrous fluid from the residual melt after the crystallisation of main pegmatitic assemblages, and that the H₂O-rich component was mobilised into country rocks.

Graphical abstract



Keywords

Leinster pegmatite belt; albite-spodumene pegmatite; pegmatite zonation; albitisation.

1. Introduction

Spodumene pegmatites constitute one of the few economic sources of lithium and may also carry significant tantalum, caesium and other rare metals. Lithium production from brines is regarded as more attractive economically due to large size of deposits and low production costs; world production, mainly in the Andes, often outstripped production from pegmatites in recent years (USGS 2019). However, although individually small, spodumene pegmatites may become increasingly attractive to mine as lithium demand increases, due to their smaller footprint and greater agility in responding to increased demand (Gunn 2014; USGS 2018).

Internal differentiation and consequent geochemical evolution in pegmatites are significant processes in the development of economically viable deposits of metal-bearing minerals. World-class pegmatitic deposits such as Tanco were formed due to extreme differentiation of granitic melt from the margins inwards, with rare minerals such as pollucite formed in the latest stage of crystallisation (London 2008). Variability of some incompatible elements including Li, Rb and Cs in minerals such as K-feldspar, micas and tourmaline may be useful tools to reveal fractional crystallisation processes in pegmatite provinces (e.g. Garate-Olave et al. 2017, Černý et al. 1981), but may also be related to variable source rocks or degrees of partial melting (e.g. Shearer et al. 1992).

Considering individual bodies, most granitic pegmatites present two distinct textural domains, according to London (2009): anisotropic textures in outer zones, and coarse and blocky textures in interior zones. This is suggested to result from liquidus undercooling in the borders, and, in the rest of the pegmatite, accumulation of network-modifying elements including B, Li, F and P in the crystal growth front until crystallisation is complete.

Main author's current address: Geological Survey of Belgium, Royal Belgian Institute of Natural Sciences, Jennerstraat 13, 1000 Brussels, Belgium

Consequently, mineralogical and geochemical changes inside pegmatite bodies are commonly traceable among different zones and can be used to understand how pegmatites evolve internally (e.g. Wise and Brown 2010). Moreover, wallrocks that are reactive to pegmatitic fluids can also be used to monitor the geochemical evolution of pegmatite bodies (e.g. Morgan and London 1987, London 2008).

Albite-spodumene pegmatites challenge the general rules of pegmatite petrogenesis. According to Černý and Ercit (2005), these rocks are characterised by dominance of albite and quartz over K-feldspar, with bulk pegmatite Li concentrations in the uppermost range obtained by experimental magmatic enrichment, around 2 wt. % Li_2O . Simple zonation is common, with nearly homogeneous pegmatite bodies, and outer zones of granitic and graphic texture are mostly absent; extensive volumes of saccharoidal or platy albite are present (Černý 1989). Because of these characteristics, they represent important resources of Li and Ta worldwide: Barroso-Alvão (Lima 2000), Cachoeira Group (Romeiro and Pedrosa-Soares 2005), Brazil Lake (Kontak 2006) and Kings Mountain (Swanson 2012) are a few examples. The factors responsible for primary fabrics of larger crystals coexisting with randomly aligned matrix are obscure and in need of detailed investigation (Černý and Ercit 2005). Although wallrock alteration around some rare metal pegmatites has been studied (e.g. Shearer et al. 1986), revealing significant geochemical haloes, the links between the processes of pegmatite crystallization and pegmatite–wallrock interaction in albite-spodumene pegmatites remain poorly understood.

In Leinster, southeast Ireland, unzoned to weakly zoned albite-spodumene pegmatites targeted for exploration provide the opportunity to investigate the internal geochemical evolution processes that result in these unusual characteristics. In addition, albite-spodumene and spatially associated barren pegmatites both contain late-stage albitite that developed after the early primary magmatic minerals. Trace element mapping of muscovite and columbite-

tantalite has revealed complex internal evolution transitioning from magmatic to hydrothermal processes (Kaeter et al. 2018). In this paper we investigate these processes further, presenting mineral scale geochemical analyses from margins inwards of zoned and unzoned spodumene pegmatite intersections. Chemical comparisons between ubiquitous minerals in pegmatites and wallrocks were studied in an attempt to achieve a complete understanding of (1) internal evolution of pegmatite bodies, (2) characteristics linked to the poor development of zonation, and (3) links between internal evolution and pegmatite–wallrock interaction.

2. Geological setting

2.1 Regional geology of the Leinster Batholith margin

The studied region is part of the Leinster Terrane. The dominant Ribband Group (Fig. 1) comprises a Lower Ordovician succession dominated by finely laminated mudstones. It has been divided into several formations (Tietzsch-Tyler and Sleeman 1994), including the Maulin Formation, which forms the immediate country rocks of many spodumene pegmatites.

The Leinster Terrane exhibits two main deformation phases: a D1 phase and greenschist facies metamorphism that generated subvertical NE-SW S1 slaty cleavage and small-scale F1 folding, and a D2 phase that generated NE-SW schistosity and large-scale F2 folding. The prominent regional deformation in the Leinster Terrane is part of the D2 phase and has been interpreted as Acadian due to the temporal correlation with the intrusion of the Leinster Batholith (Chew and Stillman 2009), although this might need revision in light of recent geochronology work discussed below. Regional-scale thrust faults and D2 sinistral shear

zones include the East Carlow Deformation Zone (ECDZ), a 3 km wide NE-SW zone along much of the eastern margin of the Leinster Batholith (McArdle and Kennedy 1985; Chew and Stillman 2009).

The ECDZ, which hosts most of the known spodumene pegmatites, is a dip-slip ductile zone with an element of sinistral shearing and is represented by the modification of S1 slaty cleavage to a penetrative S2 fabric, along with tightening of F1 folds and the development of an L2 northwest or southeast mineral lineation (McArdle and Kennedy 1985). The ECDZ affects granitic and metamorphic rocks on the margin of the Tullow Lowlands pluton (Fig. 1). Movement on the ECDZ may have begun at ~460 Ma (Fritschle et al. 2018a) and continued until the late Carboniferous (Tietzsch-Tyler and Sleeman 1994).

Granitic intrusions in the area (Fig. 1) include the Leinster Batholith, the Blackstairs Unit, and numerous smaller granitic bodies (Tietzsch-Tyler and Sleeman 1994). These were considered part of the Trans-Suture Suite (Brown et al. 2008), which straddles the trace of the Iapetus suture in Britain and Ireland. However, major granitic magmatism in south Leinster is now known to have only partly taken place after Iapetus closure, with several intrusive episodes between the Lower Ordovician (~470 Ma) and Lower Devonian (~405 Ma) (Fritschle et al. 2018a, 2018b).

The largest granitic body in southeast Ireland is the Leinster Batholith (Fig. 1), composed at least in part of sheeted intrusions of S-type two-mica granitic rocks (Grogan and Reavy 2002; Chew and Stillman 2009). It has been mapped as four plutons of granite-granodiorite. The ascent and emplacement of magma batches is thought to have been facilitated by the ECDZ (McArdle and Kennedy 1985; Tietzsch-Tyler and Sleeman 1994). The Tullow Lowlands pluton is of special interest as it hosts spodumene pegmatites (Fig. 1). It comprises equigranular and homogeneous monzogranite to granodiorite, with subordinate tonalite (Luecke 1981). It is occasionally porphyritic with K-feldspar megacrysts, and exhibits

foliated and sheeted margins interfingering with the adjacent schist (Tietzsch-Tyler and Sleeman 1994; Chew and Stillman 2009).

Leinster Batholith granitic magmatism imposed a contact aureole up to 400 m wide on the Ribband Group; rocks of the Kilcarry Member were metamorphosed to amphibolites and chlorite schists (Tietzsch-Tyler and Sleeman 1994). The development of schistosity along with porphyroblasts of sillimanite, staurolite, garnet, andalusite and biotite indicate a temperature >500 °C (Sweetman 1988; Tietzsch-Tyler and Sleeman 1994). O'Mahony (2000) showed the high-T aureole from the Leinster Batholith reached 550°C at 3-4 kbar.

2.2 Geology of the Leinster albite-spodumene pegmatite belt

Lithium pegmatite bodies of the albite-spodumene type (Černý and Ercit 2005) up to ~20 meters thick are known from at least ten localities in south Leinster, mostly located along the eastern flank of the Tullow Lowlands pluton (Fig. 1). These will be referred to as *spodumene pegmatites* for brevity from here onwards in the text. Barren granitic pegmatites, i.e. those containing mainly rock-forming minerals (i.e. feldspars, mica, quartz), are commonly found in spatial association with lithium pegmatites.

The pegmatite belt is characterised by the predominance of fibrous to lath-shaped spodumene associated with variable amounts of quartz, plagioclase, microcline and muscovite. Accessory minerals within spodumene-rich parts of pegmatites include platy black columbite-tantalite, brown cassiterite aggregates, blue manganiferous F-apatite, lithiophilite, spessartine, colorless to light green beryl, schorl and pyrite. Ubiquitous fine-grained albitite with associated quartz and yellow-greenish muscovite was described by various of these authors (Steiger and von Knorring, 1974; Whitworth and Rankin, 1989). Often referred to as aplite, this rock type was interpreted as the pegmatite border zone,

although this is likely to be replacive albitite, as discussed later. Internal zonation in some spodumene pegmatites was recognised by Whitworth and Rankin (1989), although not characterised in detail.

Country rocks of the Leinster Batholith and the Maulin Formation were described by McArdle (1984), McArdle and Kennan (1987) and Whitworth (1992). The region is marked by garnet and staurolite-bearing mica schists and tourmalinites of the Ballybeg Member, muscovite-chlorite-tourmaline-biotite-garnet schists and hornfelses with accessory tourmaline and pyrite, along with minor tourmalinite and psammite bands of the Monaughrim Member, and hornblende-biotite-chlorite schists of the Kilcarry Member. Coticule layers with spessartine porphyroblasts within a quartz and muscovite matrix are also common in the sequence. Tourmaline is notably present close to the pegmatite contact in Aclare schists.

Some authors (Whitworth and Rankin 1989; O'Connor et al. 1991; Whitworth 1992) suggested pegmatites evolved from a late-magmatic / early-hydrothermal fluid developed from the Leinster Batholith and then cooled isobarically until crystallisation. It was assumed that pegmatites and granite were then altered by a late hydrothermal fluid generated from the metamorphic country rocks. Other authors (McArdle and Kennan 1987) suggested lithium and other uncommon elements present in volcanogenic exhalative sediments of the Kilcarry Member prior to granite emplacement were remobilised into spodumene pegmatites when granitic magmas intruded. McArdle and Kennan (1992) proposed a direct anatectic origin for rare-element pegmatite melt with these rare-element-rich sediments as protoliths. More recently, the origin of pegmatites by partial melting of metasedimentary rocks has been modelled geochemically and origin by fractionation of granitic magma discounted (Barros and Menuge 2016).

3. Methodology

3.1 Sampling and petrography

The description of rock types and textures, and sampling to characterise pegmatite bodies and country rocks, was mostly carried out from in situ occurrences intercepted by drill cores from localities Aclare and Moylisha (Fig. 1), part of the ongoing exploration campaign of Blackstairs Lithium Ltd. since 2011. Samples studied in this paper come from two shallow to moderate dip drill cores from Aclare, ACL 13-02 (four spodumene pegmatite intersections) and ACL 13-04 (three spodumene pegmatite intersections), and one drill core from Moylisha, MOY 13-03 (two spodumene pegmatite intersections). Lithologies intercepted by these drill cores are represented in Fig. 2. Drill cores ACL 13-02 and ACL 13-04 represent the thickest intersections of lithium pegmatite (10 to 20 m) and highest Li grade among drilled pegmatites (estimated as ~2.2 wt.% Li_2O by Blackstairs Lithium Ltd.). MOY 13-03 presents the highest Li grade in Moylisha (estimated as ~1.5 Li_2O % by Blackstairs Lithium Ltd.). This drill intercepted two spodumene pegmatite intersections 12 m thick and 5 m thick, and several barren pegmatite intersections of variable thickness (tens of cm to a few m).

Thirty-five polished sections were made from representative samples from mineralised and barren pegmatites and their wallrocks (Fig. 2). These were initially characterized with a Nikon Eclipse LV100POL polarizing optical microscope, using transmitted and reflected light, and a Hitachi TM-1000 scanning electron microscope in the School of Earth Sciences, University College Dublin, Ireland.

3.2 Whole-rock analyses

Whole-rock geochemical analyses were obtained for pegmatites, hanging wall and footwall (country rocks to pegmatite intrusions) as part of the exploration campaign. The three drill cores were each split in half and divided into lithologically homogeneous parts, between 7 cm and 3.05 m long, resulting in 124 samples. These parts were then crushed, decomposed by four acid digestion and analysed for 48 elements by ICP-MS by ALS Minerals (Loughrea, Co. Galway, Ireland). Routine practices were used to ensure data quality control: sample duplicates (1 in every 20 samples), homogeneous quartz pebbles (1/40) and certified standards (1/20). Results showed reproducibility between duplicates within 15% for most elements and no contamination problems. Detection limits for the elements analysed range between 0.02 and 100 ppm.

The volumes of the samples analysed are considered representative to estimate the whole-rock geochemistry of Leinster pegmatites, considering their typical “fine” grain size around 2 cm and negligible variations in pegmatite mineralogy among drill cores, boulders and outcrops of the same locality. Furthermore, it is assumed that the drill core samples are representative of the pegmatite bodies from border to border and that each pegmatite body crystallised from a single batch of evolving melt, as discussed by Barros and Menuge (2016) and Kaeter et al. (2018).

3.3 Electron microprobe analysis (EPMA)

Minerals of distinct zones in mineralised and barren pegmatites were analysed with a Cameca SX 100 electron microprobe at the Joint Laboratory of Electron Microscopy and Microanalysis of the Department of Geological Sciences, Masaryk University, Brno, Czech Republic. Analyses were carried out in wavelength-dispersive mode and accelerating voltage of 15 kV, beam current of 10 or 20 nA and spot sizes between 1 and 7 μm .

Major elements were each measured for 10 to 20 s and the minor and trace elements for 40 and 60 s, respectively, on the peak, and ½ of the peak times for background counts on both sides of the peak. Raw data were converted into concentrations using appropriate X-PHI matrix corrections (Merlet 1994).

Formulae of the major, and some minor, mineral constituents of pegmatites from two localities, Aclare and Moylisha, as well as some minerals in and outside the exocontact in country rocks, were calculated based on EPMA analyses. Details of the assumptions and calculations used can be found in Supplementary Table 1.

Data for barren pegmatites is presented in the supplementary material and mentioned in the text for comparison, but not represented in the figures or discussed in the model since it is beyond the scope of this study.

4. Results

4.1 Macroscopic features of pegmatites and their wallrocks

Basic information on mineralogy and texture of spodumene pegmatites and country rocks in the three drill cores samples is given in Table 1. Barren pegmatites are described separately below.

The Aclare spodumene pegmatite intersections include a thin upper border zone (Fig. 3B), followed inwards by a far thicker spodumene interval (Figs 3C and D). Here, spodumene habit varies from subhedral short to elongate prisms or laths; elongate crystals may be deformed and/or broken (Fig. 3C) and no preferred orientation is consistently observed away from borders, as elongate crystals may be parallel, oblique or perpendicular to the contact plane. Spodumene crystals are often partially or fully altered to dark green fine-

grained mica (Fig. 3B). Occasional replacive coarse quartz-muscovite assemblage occurs within Aclare pegmatites, which has been characterised in detail by Kaeter et al. (2018) but is mostly absent in the intersections analysed for this study. The spodumene pegmatite intersections in Moylisha are in irregular upper and lower contact with the foliated porphyritic granodiorite, at high angles to the foliation (Fig. 4D). No border zone is identified, and spodumene occurs at the contact with wallrocks (Figs 4C and D). The lower contact with porphyritic granodiorite on the footwall is dominated by the spodumene-bearing assemblage (Fig. 4C).

Spodumene crystals are occasionally partially replaced by green mica, quartz and/or overgrown by fine-grained material, often with a saccharoidal texture in hand specimen, hereafter named saccharoidal albite; the term albitite was introduced by Kaeter et al. (2018) for this facies. It is composed of >80% albite, minor quartz and muscovite and numerous accessory minerals. Elongate prismatic albite, and elongate quartz when present, are often oriented subparallel to the main foliation of the wallrocks and pegmatite-wallrock contacts. Oriented crystals are observed both in interstitial patches of albitite between coarse crystals and in larger volumes of albitite (Figs 3B and F). Notable accessories include lithiophilite, which may be occasionally elongated and is more abundant at Moylisha, especially towards lower contacts where it has a fracture-filling habit (Figs 4E and F). The amount of albitite is variable throughout the intersections but at Moylisha tends to be more abundant towards lower contacts. Even though no spodumene is identified, some of the green mica is similar to the mica in spodumene pseudomorphs, and these intersections may represent fully altered spodumene pegmatite. Saccharoidal albite never occurs within wallrocks around spodumene pegmatites.

The thickest pegmatite intersection from ACL 13-04 is the only one to show a clear core zone, with an abrupt and irregular change ~10 m below the upper border from the

spodumene-bearing interval to an assemblage of massive K-feldspar with associated green muscovite-rich, quartz-rich and radiating plagioclase-rich portions (Fig. 3E). The ~2.5 m thick core zone is spodumene-free and has associated interstitial albitite including some cassiterite. The lower spodumene-bearing interval of the lowest intersection is similar to the upper spodumene-bearing interval, except that albitite patches are more abundant (Fig. 3F) and spodumene pseudomorphed by dark green mica is common. A possible strongly albitized quartz core zone is also present in one of the Moylisha intersections.

The wallrocks of both spodumene and barren pegmatites are mostly varieties of granite, except for the hangingwall of the uppermost spodumene pegmatite intersection at Aclare, which is mica schist (Fig. 3A). The granitic wallrocks include the Tullow Lowlands pluton Type II granite and minor granitic intrusions, both broadly of granodioritic composition. The portions of host rock that are chemically changed by pegmatites, and consequently present different mineralogy, will be called exocontact throughout the text. Exocontacts include narrow zones adjacent to pegmatites whose mineralogy and texture are different to unaltered host rocks (e.g. Fig. 3G).

Xenoliths of mica schist (~2 cm) and foliated granodiorite (~2 to 15 cm) are common within Aclare spodumene pegmatites, and here higher apatite megacryst abundance or development of a discrete border zone and comb textures of spodumene pseudomorphs may be present. Altered wallrock xenoliths are also common at Moylisha near the contact surfaces with foliated porphyritic granodiorite (Fig. 4F).

Barren pegmatites are hosted by the foliated granodiorite at Moylisha and are unzoned, coarse-grained (typical crystal size 4 cm, maximum 10 cm) and consist of blocky feldspars (20-50%), quartz (20-35%), muscovite (15-20%) and garnet (2-5%). Feldspars occur as subhedral to euhedral tabular crystals, along with early euhedral dark orange garnet, that is predominant in the borders, and later quartz and muscovite. Contacts with host granitic rock

are irregular and can be diffuse or abrupt, at variable high angles to the foliation (e.g. Fig. 4A), and elongate quartz crystals at the border may be aligned within the same plane. This primary pegmatitic assemblage is altered by fine-grained saccharoidal albitite comprising albite (80%), quartz (5%) muscovite (5%), garnet (5%) (Fig. 4B) and minor beryl and apatite. The alteration occurs as patches within coarse-grained primary minerals and does not crosscut the granitic host rocks.

4.2 *Whole-rock compositions*

Whole-rock concentrations for a series of major and trace elements in pegmatites and wallrocks are presented in Supplementary Table 2. The ratio K/Rb is used to monitor the Rb enrichment in pegmatites and country rocks, which will be mainly controlled by biotite (wallrocks only), muscovite (all) and K-feldspar (all). Both wallrock types have low Rb, resulting in high K/Rb ratios of >90. The enrichment in Rb, Li, Cs and Ta in samples from wallrocks represents spodumene pegmatite exocontact samples, not extreme fractionation (Fig. 5). Data for the zoned spodumene pegmatite (ACL 13-04) (Fig. 5A) shows evolution from ~1000 ppm Li and ~100 ppm Cs in the border zone to a maximum of ~10000 ppm Li and ~200 ppm Cs in the spodumene zones, followed by decrease in both elements in the core zone, while K/Rb (and Rb concentration) remains approximately constant, below 30. Unzoned spodumene pegmatites (ACL 13-02 and MOY 13-03) (Figs. 5B and C) show a similar trend, with additional decrease in Li and Cs in samples from the saccharoidal alteration. In albitised samples in Moylisha the highest Ta (and Ta/Nb) is recorded (~2). Values for Nb and Ta remain roughly constant around 1.

4.3 *Microscopic observations and mineral chemistry*

4.3.1 Feldspars

K-feldspar and albite are major constituents in both spodumene and barren pegmatites and country rocks, and their chemistry is presented in Supplementary Tables 3 and 4, respectively. Blocky K-feldspar and plagioclase are present in spodumene pegmatite as primary minerals (Fig. 6A), and late fine-grained platy albite is widespread, replacing K-feldspar and spodumene, or K-feldspar only in barren pegmatites. The fine-grained albite is often present in veinlets (Fig. 6B) and might record flow textures (Fig. 6C) and relics of K-feldspar and irregular spodumene rims are common within larger volumes of saccharoidal albite (Fig. 6D). In granitic country rocks, K-feldspar is often represented by megacrysts, and in the groundmass the mineral is less abundant than plagioclase and is often interstitial. In mica schist, K-feldspar and plagioclase occur in bands parallel to the main foliation.

K-feldspar composition in all rock types has predominant orthoclase component ($>87\%$), with variable albite (2-12%) and little anorthite ($<0.2\%$). Minor elements are distinct among country rocks and barren pegmatites versus spodumene pegmatites, as the last are commonly enriched in P (<0.002 apfu in country rocks and barren pegmatites versus up to 0.020 apfu in spodumene pegmatites), Rb (none versus up to 0.018 apfu) and Cs (none versus up to 0.003 apfu). Rb and Cs contents increase moderately from granitic country rock to barren pegmatites, and sharply in spodumene pegmatites, with highest concentrations in crystal rims (Fig. 7A). One core zone K-feldspar analysis yielded a low total of 97.5 wt%, which could indicate H_2O or $(\text{NH})^{4+}$ substitution for K^+ .

Plagioclase is almost pure albite in spodumene and barren pegmatites ($\text{An}_{<2.3}$), with the exception of a border zone plagioclase with An_{21} , while in wallrocks oligoclase is dominant (An_{10-30}); anorthite contents decrease in pegmatite exocontacts in granitic rocks and both Na-

and Ca-enriched rims are observed (Fig. 7B). In spodumene pegmatites, minor constituents include Rb (<0.004 apfu), P (<0.010 apfu) and Fe (<0.002 apfu); Rb and Fe may reach higher values in the exocontact in granitic rocks (~0.005 apfu for both). In pegmatites, no major geochemical difference can be identified between coarse, presumably early primary, and late fine, saccharoidal albite in different bodies or zones (Fig. 7B). One border zone albitite albite analysis and one spodumene interval albite analysis yielded high totals (>101.0 wt%). Two albitite albite compositions yielded low totals (<98.0 wt%), which could indicate the presence of undetectable components such as H₂O.

4.3.2 Micas

Micas (Supplementary Table 5) in pegmatites are predominantly muscovite; in host rocks biotite also occurs and is often altered to chlorite. Pegmatitic muscovite is coarse-grained (>5 mm) and usually homogeneous in terms of major elements. Muscovite associated with albitite in both pegmatite types is finer-grained and homogeneous. Muscovite in the spodumene pegmatite exocontact in mica schist and granodiorite frequently presents complex textural patterns with associated biotite and siderophyllite. Some low molecular totals (95-97.9%) are likely due to uncertainties in the estimation of Li₂O and H₂O.

Muscovite presents little chemical variation within the pegmatite intersections studied, with a few samples showing rims (Fig. 6E) of polyolithionite composition (Fig. 8A). This is chemically similar to fine-grained mica produced by spodumene alteration (Fig. 6E). A similar trend of compositional change is observed in muscovite in the spodumene pegmatite exocontact in country rocks (Fig. 8A). Biotite in the exocontact lies within the siderophyllite compositional range, probably after phlogopite–annite (Fig. 8A).

Some element concentrations in muscovite are notably higher in country rocks and barren pegmatites when compared to spodumene pegmatites, e.g. Mg (0.10-0.72 apfu in mica schist and granodiorite adjacent to pegmatites, 0.06-0.08 apfu in barren pegmatites and <0.04 apfu in spodumene pegmatites), Ti (>1 wt. % TiO₂ in country rocks <0.1 wt. % in spodumene pegmatites) and Fe (Fig. 8A). Considering the most abundant minor elements, muscovite in spodumene pegmatites is enriched in Rb and Cs when compared to most country rock samples, with Cs reaching over 1000 ppm (Fig. 8B and C). However, enrichment in those elements is also observed in the exocontact in some mica schists and granitic rocks (Fig. 8B and C).

4.3.3 Spodumene

Spodumene can make up to 40% volume of pegmatites and is the main host of Li in spodumene pegmatites. Crystals are usually subhedral short prisms, often with altered rims when in contact with albitite (Fig. 6D and E). Its chemistry varies little, generally being close to the ideal formula LiAlSi₂O₆ (Supplementary Table 6). It should be noted that calculations yield high molecular totals (up to 102.1%), but still within acceptable error limits considering uncertainties in the determination of Li. The small amounts of impurities present consist mainly of Fe (<0.012 apfu), and lesser Na, Rb and Ca. Iron and Mn contents tend to decrease from pegmatite border zones inwards and Fe tends to decrease from crystal cores to rims (Fig. 9). Spodumene relics in the albitite contain relatively high Na (~0.008 apfu).

4.3.4 Garnet

Garnet (Supplementary Table 7) is a common accessory mineral in spodumene and barren pegmatites, and also occurs in the host schist. In spodumene pegmatites, garnet crystals are coarse-grained (>3 mm), subhedral to anhedral, and intergrowth with spodumene and/or apatite is common (Fig. 6F). Garnet is more abundant in barren pegmatites and associated albitite, and crystals are finer-grained and often euhedral or subhedral, with regular zonation and spatially irregular chemical variation both common features. In the mica schist, pre- to syn-deformation garnet porphyroblasts are common, usually with poikiloblastic core and inclusion-free rims.

Calculations yielded oxygen sums very close to 12, indicating negligible Fe^{3+} . Garnet in spodumene pegmatites is the most enriched in Mn (~2 apfu or more) and depleted in Fe and Ca (<1 apfu), so is always spessartine (Fig. 10A). In barren pegmatites and mica schist, Fe is predominant (>1.5 apfu) (Fig. 10B) and therefore corresponds to Mn-rich almandine, except for one garnet crystal in a schist xenolith in the border zone of spodumene pegmatite, which has low Fe and high Mn. Depletion in Mn and Ti and increase of Fe is observed from cores to rims (Figs. 10A and C).

4.3.5 Beryl

Beryl (Supplementary Table 8) is present in two generations in spodumene pegmatites: an early generation present in the spodumene zone and a late generation in saccharoidal albite. In barren pegmatites, beryl occurs only in saccharoidal albite. Early beryl crystals are pale yellow-green, medium- to coarse-grained and irregularly zoned (Fig. 6G). Beryl in the albitite is often anhedral and poorly zoned, with occasional alteration to bertrandite. Beryl is also present as a minor poikilitic phase within the immediate spodumene pegmatite exocontact in mica schist, associated with the tourmalinisation.

Of the minor constituents of beryl, relatively high Na is common (up to 0.317 apfu), along with high Li in spodumene pegmatites (estimated at ~0.8 apfu), considerable amounts of Cs (up to 0.036 apfu), Fe (< 0.031 apfu) and Rb (< 0.009 apfu), and trace Zn, K, Mn and Ca (all <0.007 apfu). The chemistry of beryl in the schist is similar to the phase present in spodumene pegmatites (Figs. 11A and B). Beryl in spodumene pegmatite is enriched in Cs, and slightly in Na towards rims, while in saccharoidal albite associated with barren pegmatite, comparatively low Na and Cs, and high Fe, are observed (Figs. 11A and B). Low totals for three analyses (97.5-97.8%) probably reflect limitations in the estimation of Li₂O and BeO or partial alteration of beryl to betrandite.

4.3.6 Apatite and lithiophilite

Fluorapatite (Supplementary Table 9) is a common accessory mineral, often hosting U-rich and Fe-rich inclusions in spodumene pegmatites. Lithiophilite (Supplementary Table 10) fills fractures and crystal boundaries in albitite, being more common in Moylisha spodumene pegmatites. Granitic apatite is Mn-poor and metamorphic apatite in mica schist is fine-grained, free of inclusions and elongated along the foliation.

Apatite in spodumene pegmatites is enriched in Mn (up to ~1 apfu) substituting for Ca, and, on average, Na (up to ~0.2 apfu) when compared to apatite in country rocks. Minor elements present include Fe (<0.05 apfu) and LREE, Sr, Mg, Ba and Th (<0.02 apfu). Some enrichment in Y is observed in the spodumene pegmatite exocontact in country rocks (up to ~0.02 apfu), while it is almost undetectable in pegmatites. Apparent excess F beyond the stoichiometric maximum (2 apfu) is common in the majority of apatite analyses and is caused by the time-dependent variation of the halogen X-ray counts in apatite (Stormer et al. 1993; Goldoff et al. 2012; Stock et al. 2015). The fine-grained nature of randomly oriented

crystallites does not allow proper F determination. Lithiophilite has higher Fe/Mn in Aclare when compared to Moylisha; all analysed crystals contain minor LREE, Ca and F (<0.03 apfu). One high computed total (102%) probably reflects limitations in the estimation of Li_2O .

4.3.7 Tourmaline

Tourmaline (Supplementary Table 11) is only present in the exocontact of spodumene pegmatite (Fig. 6H) within foliated granodiorite and mica schist. It belongs to the alkali group with predominant (Na + K) exceeding Ca and minor to intermediate X-site vacancies (Fig. 12A). Its composition ranges between schorl and dravite to oxy-schorl, and enrichment in Fe is observed from core to rim of all crystals analysed (Fig. 12B), sometimes accompanied by enrichment in Li.

4.4 *Mineral assemblage in weakly zoned intersection*

The major ubiquitous early primary minerals phases K-feldspar, spodumene, plagioclase and muscovite have limited geochemical variations in the weakly zoned intersection of drill core ACL 13-04 (Fig. 13). Muscovite records increases in Rb, Na, F and Cs from footwall to hanging wall inside the pegmatite, and muscovite in wallrocks shows the highest contents of Cs (Fig. 13A). K-feldspar shows a minor decrease in Rb, Na and Cs from margins to core of the intrusion (Fig. 13B). Minor elements show little variation in plagioclase and spodumene throughout the intersection (Figs. 13C and D).

5. Discussion

5.1 *Internal geochemical evolution of pegmatite bodies*

The Leinster spodumene pegmatites are mineralogically and texturally heterogeneous, but in most studied occurrences no distinctive mineralogical zonation as described in the literature (e.g. Whitworth and Rankin 1989) can be identified. Typical graphic textures or border zone banded aplite are mostly absent, and it is possible that the term aplite was applied by previous authors to quartz-bearing late primary albitised parts of pegmatites. Pegmatite bodies seem to be composed of a single spodumene-bearing interval similar to the spodumene zone of the zoned Aclare intersection, likely equivalent to the intermediate zone of Cameron et al. (1949). The only (poorly) zoned Aclare intersection is also the thickest (Figs 2 and 13), and the volume of initial melt could be a controlling factor in development of zonation in Leinster.

According to the general crystallisation process proposed by Kaeter et al. (2018), the evolution in Leinster pegmatites can be subdivided into three stages: magmatic, with early primary K-feldspar, spodumene, quartz, albite and muscovite (\pm garnet, beryl and other minor phases); transitional, with at least muscovite, quartz and columbite-group minerals (CGM) crystallising; and hydrothermal, with predominant albitite (\pm garnet, beryl, apatite, CGM and other minor phases). These are detailed below and represented in Fig. 14.

5.1.1 Magmatic stage

The presence of primary spodumene and quartz indicates a Si-saturated crystallising environment. The absence of primary petalite or evidence of petalite breakdown (sqi) indicate Leinster pegmatites crystallised in the conditions of the spodumene stability field (London

2005) at pressures of at least ~150 MPa and maximum temperature of ~725 °C. This is equivalent to depths greater than 4-5 km.

Experimental work by Maneta and Baker (2014) and Maneta et al. (2015) showed pegmatite-forming melts may accumulate thousands of ppm Li above saturation before the crystallization of Li-aluminosilicates. Pegmatite bodies formed by Li-supersaturated melts are expected to have abundant Li-aluminosilicates in proximity with the wallrocks (Maneta et al. 2015). These textural characteristics are observed in Leinster as spodumene is at, or within a few centimetres of, the contact surfaces with wallrocks (Figs. 3B, 4C and D), strongly suggesting Li-saturation prior to crystallisation, and possibly supersaturation as evidenced by the aforementioned experiments. Lithium saturation prior to crystallisation could cause spodumene nucleation throughout the thickness of pegmatite magma bodies at once, which could explain homogeneously distributed and typically randomly oriented spodumene crystals observed in Leinster and other albite-spodumene pegmatites. The presence of primary muscovite also suggests the initial melt was H₂O-rich. The highly evolved initial composition is one possible cause for the weak to absent zonation. Thin (< 1 cm) albite-rich margins in other intersections of Leinster pegmatites are not considered border zones *sensu stricto*.

The chemistry of early primary (Fig. 14A, Stage 1) minerals in pegmatites shows that limited geochemical fractionation took place in crystallising bodies: increase in incompatible elements from core to rim is observed in K-feldspar (e.g. Rb), beryl (e.g. Cs) and muscovite (e.g. Cs and Rb); the same is true for the composition of these minerals throughout the weakly zoned intersection. Manganese substitution in apatite indicates a reduced crystallising system, which is expected for such geochemically evolved felsic melts (Belousova et al. 2002). Contents of Mn in apatite increase from core to rim of crystals and are generally higher in crystals within the albitised pegmatite. These observations confirm that even if the

starting point is a highly evolved melt and zonation is absent or not pronounced, some magmatic fractionation is identifiable. However, increasing $\text{Fe}^{2+} = \text{Mn}^{2+}$ substitution towards rims of spessartine crystals (up to 40 n/n% almandine) indicate an opposite trend.

With the onset of solidification and spodumene crystallisation, Li concentrations in the crystallising melt are expected to drop; P, H_2O , B and F are mostly incorporated in accessory minerals, so these are likely to remain at high concentrations in the crystallising melt, enabling high diffusion rates and consequent pegmatitic textures (London 2009). Rubidium is substantially incorporated in K-feldspar and muscovite, and concentrations in the residual melt are also expected to drop during magmatic crystallisation. The crystallisation advances until an incomplete interconnected crystalline framework is reached, which is supported by the presence of K-feldspar in the core zone of ACL 13-04; the absence of spodumene or other Li-minerals in this core zone suggests Li concentrations reached a minimum at that stage. The limited geochemical fractionation indicates this is not the main factor for development of zones in pegmatites crystallising from highly evolved initial melts. Other factors including volume of initial melt and thickness of crystallising body should also be considered.

Although F is usually not detectable in early primary minerals except accessory F-apatite, tourmaline and F-rich micas are observed in exocontacts. Therefore, it is assumed that B and F were present, but not saturated, in the initial melt. Caesium, present as a trace component in primary minerals, is also assumed to have been present in the initial melt below saturation, and partially incorporated in muscovite. Trace Cl in most primary minerals indicates this element was also present in the initial melt.

5.1.2 Magmatic-hydrothermal transition

The silicic residual melt after the crystallisation of Stage 1 minerals in Leinster is thought to be relatively enriched in the most incompatible elements not yet substantially incorporated into any minerals (e.g. Cs, Ta, Nb, other HFSE), with increased Na/K (as K-feldspar is dominant over plagioclase in the primary assemblage), elevated H₂O and some Rb, Be, F and Cl, but minor Li. Also, the interstitial melt has increased concentrations of network modifiers such as P, B, which probably delay its crystallisation and decrease its viscosity (e.g. Bartels et al. 2011; London and Morgan 2012), and possibly increase its reactivity.

The composition and low viscosity of the residual melt turns it into a reactive and pervasive melt-fluid, possibly characterised by two immiscible melts due to cooling (c.f. Thomas and Davidson 2016). Dissolution of primary crystals, specially K-feldspar and spodumene, starts in response to the melt-fluid interaction (e.g. Fig. 6D). This is interpreted to be a record of the internal changes related to the transition (Fig. 14B, Stage 2) from magmatic to hydrothermal crystallisation. At this stage, partial dissolution of spodumene and K-feldspar will cause reincorporation of Li and Rb in the residual melt, causing concentrations to rise again. Furthermore, Ca and P are released from primary feldspars. Liberation of the network builders Si and Al might increase the polymerisation of the melt-fluid again, which could explain oscillations between crystallization from polymerised melt and melt-fluid observed by Kaeter et al. (2018). Similar pervasive replacement textures have been described by Kontak (2006). Orville (1963) has showed fluid-mediated exchange of Na for K takes place in cooling environments.

5.1.3 Hydrothermal stage

The early primary mineral assemblage is often crosscut and replaced by saccharoidal albite (e.g. Fig. 6B-D). This is a common feature in poorly zoned spodumene pegmatites elsewhere

and is now recognised globally as a common late-stage texture of magmatic crystallisation (e.g. Demartis et al. 2014; Dewaele et al. 2011; Galliski et al. 2012; Hulsbosch et al. 2013; Kontak and Kyser 2009). This material may at least partially replace pre-existing K-feldspar, spodumene and other early primary minerals (e.g. Cameron et al. 1949; Kontak and Kyser 2009). Saccharoidal albite may be a fine-grained version of cleavelandite (Fisher 1968), which might have led to it being previously described this way (Steiger and Von Knorring 1974).

The saccharoidal albite in Leinster pegmatites represents hydrothermal (Fig. 14C, Stage 3) crystallisation and albitisation. It has minerals in common with the Stage 1 assemblage, including albite, muscovite, garnet, apatite and beryl, and an increase in modal lithiophilite, CGMs, sphalerite and cassiterite, indicating enrichment in incompatible elements including Ta and Sn with ongoing crystallisation (Kaeter et al. 2018). The sodium-rich environment seems to cause limited $\text{Na}^+ = \text{Li}^+$ substitution in spodumene to jadeite ($\text{NaAlSi}_2\text{O}_6$), as noted by increased Na in spodumene relics within hydrothermal albitite. This has been observed for other albite-spodumene pegmatites (Filip et al. 2006). The extent of albitisation can be extreme, causing all spodumene to be consumed locally, e.g. the deepest pegmatites in drill core ACL 13-02 (Fig. 2).

Similar geochemical and mineralogical features between saccharoidal albite and host pegmatite, and sodic metasomatism by highly volatile, residual pegmatite fluid restricted to pegmatites (without albitisation of wallrocks), suggest that the albitisation results from residual liquids after fractional crystallisation of highly-evolved pegmatite melt, and not from external influx of fluids or secondary alteration. These observations are in agreement with assumptions by Černý and Ercit (2005) that albite-spodumene pegmatites represent the highest degree of regional geochemical fractionation from a granitic source. It also supports

the idea that alteration of spodumene to albite is a normal consequence of rare-element pegmatite cooling in a closed system (Wood and Williams-Jones 1993).

Alternatively, however, albite-spodumene pegmatites could represent small batches of geochemically-evolved, H₂O-bearing partial melts that, once partially crystallised, generate residual hydrothermal fluids. Abundance of albitisation in spodumene pegmatites such as the occurrences in the Leinster belt could therefore indicate that lithium-supersaturated melts provide ideal conditions for residual albite formation.

5.2 Mechanism and timing of pegmatite-host rock interactions

The H₂O-rich Stage 3 fluid is the major sink for elements such as Li and Rb that are liberated from spodumene and K-feldspar breakdown. Textural, whole-rock and mineral geochemical evidence suggest that this fluid escaped from the crystalline framework through fractures and along grain boundaries, causing wallrock alteration and occurrence of tourmaline, Cs-, F-, Rb-, Li-enriched micas and minor beryl in exocontacts (Figs. 3A and G; 5; 6H). The presence of minerals enriched in elements such as Li, Rb, F and B (siderophyllite, tourmaline) in spodumene pegmatite exocontacts in both mica schist and granitic rocks (Fig. 5) suggests that the mobilisation of pegmatitic fluids into country rocks happened after partial resorption of the early assemblages in spodumene pegmatites at some point during the hydrothermal stage. This is clear when considering muscovite geochemistry, as the mineral in the exocontact matches the Rb and Cs contents in highly evolved pegmatitic muscovite (e.g. Fig. 8B and C). Macroscopic textural evidence of fluids entering the country rocks is infrequent, usually as feldspars + mica \pm apatite veinlets, but this might nevertheless be a common feature hidden by the lack of exposure of pegmatite contacts.

The enrichment of Li and B in exocontacts is consistent with the absence of major Li- and B-bearing phases in the core zone and albitite (Fig. 5), and presence of tourmaline and siderophyllite in the exocontact, these two minerals being the main mineralogical evidence of interaction between spodumene pegmatites and country rocks. This suggests that part of the residual Stage 3 fluid generated by pegmatite crystallisation was mobilised into country rocks through fracturing. Tourmaline core to rim evolution from dravite to Al-rich schorl may reflect progressive biotite breakdown in the exocontact, suggesting that the phlogopite component was less stable than the annite component. Alteration of exocontact biotite to siderophyllite within the pegmatite exocontact may have followed after B was removed from the fluids. Both are consistent with the increase in modal biotite (altered to chlorite) further from spodumene pegmatites.

The escape of H₂O-rich fluids from pegmatites is a possible trigger for the onset of crystallisation of the residual liquid remaining within the crystalline framework, as suggested by London (1987). The presence of F might be one of the factors displacing the minimum in the quartz-albite-orthoclase system towards the Ab apex (Manning 1981), so when this residual liquid finally crystallises it is expected to be Ab-dominated. HFSE-bearing minerals, beryl and F-rich late-stage muscovite are also precipitated.

There is possible evidence for interaction with fluids external to pegmatite bodies after their complete, or nearly complete, crystallisation. Post-crystallisation alteration is associated with fractures within albitite and includes bertrandite (after beryl), minor calcite and fluorite, and minor uraninite, microlite, and wodginite (e.g. Kaeter and Menuge 2017). The action of late metasomatism is interpreted as limited, not implying major geochemical changes in the system. However, the presence of late Ca-rich phases, possibly including some apatite, could be evidence for fluid exchange with the country rock, and may represent a late Ca enrichment

(Martin and De Vito 2014) resulting from the interaction between fluids released from pegmatites and Ca-bearing plagioclase of country rocks.

6. Conclusions

- (1) Leinster pegmatites present mineralogical, textural and geochemical characteristics coherent with Li-saturation, and possibly supersaturation, prior to crystallisation.
- (2) Leinster pegmatites show weak contact to centre zonation, and only in the thickest bodies. This can be attributed to geochemically evolved initial magma, likely leading to near simultaneous crystallisation throughout the magma body and leading to limited internal geochemical fractionation from core to edge of intrusions.
- (3) Effects of pegmatite thickness, wallrock type, deformation and consequent extent of volatile loss on weak development of zonation still cannot be discarded and need to be further investigated.
- (4) Fluids that cause sub-solidus albitisation result from fractional crystallisation of pegmatite melt and albitisation seems to be particularly favoured by highly-evolved starting melt.
- (5) Increased abundance of minerals bearing highly incompatible elements (e.g. CGM and cassiterite) and network modifiers (e.g. phosphates) in the saccharoidal albitite, as well as textural evidence, support the formation of this unit from the residual pegmatite liquid.
- (6) Albitisation implies loss of Li from the pegmatite because spodumene is resorbed without reprecipitation of major hosts for Li. A higher proportion of albitisation may indicate a higher proportion of Li lost from the pegmatite.
- (7) Enrichment in incompatible elements B, Li, Rb, Cs and F in spodumene pegmatite exocontacts in both mica schist and granite country rocks suggests unmixing of a hydrous

fluid from the residual liquid after the crystallisation of the main pegmatitic assemblages, and that the hydrous fluid was mobilised into country rocks.

Acknowledgements

The authors would like to thank Tom Culligan and Greg Van den Bleeken for the thin sections; the staff of Aurum especially Mark Holdstock and Emma Sheard; the staff of Blackstairs Lithium Ltd. especially John Harrop and Patrick McLaughlin; Petr Gadas and Milan Novak from Masaryk University Brno for help with data acquisition and discussions. The authors also thank Dr Xian-Hua Li for the editorial handling and reviews by Dr Bernard Bonin and one anonymous reviewer that significantly improved an earlier version of this manuscript.

This work was supported by the Coordenação de Aperfeiçoamento de Pessoal de Nível Superior (CAPES) [grant number 99999.009548/2013-00] for RB. This publication has emanated from research supported in part by a research grant from Science Foundation Ireland (SFI) [grant number 13/RC/2092] and co-funded under the European Regional Development Fund. The research was supported by grant GAČR 19-05198S for RŠ.

References

- Barros R., Menuge J.F. 2016. The origin of spodumene pegmatites associated with the Leinster Granite in southeast Ireland. *The Canadian Mineralogist* 54, 847-862.
- Bartels A., Vetere F., Holtz F., Behrens H., Linnen R.L. 2011. Viscosity of flux-rich pegmatitic melts. *Contributions to Mineralogy and Petrology* 162, 51-60.
- Belousova E.A., Griffin W.L., O'Reilly S.Y., Fisher N.I. 2002. Apatite as an indicator mineral for mineral exploration: trace-element compositions and their relationship to host rock type. *Journal of Geochemical Exploration* 76, 45–69.

- Brown P.E., Ryan P.D., Soper N.J., Woodcock N.H. 2008. The Newer Granite problem revisited: a transtensional origin for the Early Devonian Trans-Suture Suite. *Geological Magazine*, 145(2), 235-256.
- Cameron E.N., Jahns R.H., McNair A.H., Page L.R. 1949. Internal structure of granitic pegmatites. *Economic Geology Monograph* 2, 115 p.
- Černý P. 1989. Characteristics of pegmatite deposits of tantalum. In: Möller P., Černý P., Saupé F. [eds] *Lanthanides, Tantalum and Niobium*. Society for Geology Applied to Mineral Deposits, Special Publication 7. Springer, Berlin, pp 195-239.
- Černý P., Ercit T.S. 2005. The classification of granitic pegmatites revisited. *The Canadian Mineralogist*, 46(6), 2005-2026.
- Černý P., Trueman D.L., Goad B.E., Ferreira K. 1981. The Cat Lake–Winnipeg River and the Wekusko Lake pegmatite fields, Manitoba. Manitoba Mineral Resources Division, *Economic Geology Report* ER80–1, 216p.
- Chew D.M., Stillman C.J. 2009. Late Caledonian orogeny and magmatism, in: Holland, C.H., Sanders, I. (Eds.) *The geology of Ireland*, 2nd edition. Dunedin Academic Press, Edinburgh, Scotland, 143-173.
- Demartis M., Melgarejo J.C., Colombo F., Alfonso P., Coniglio J.E., Pinotti L.P., D'Eramo F.J. 2014. Extreme F activities in late pegmatitic events as a key factor for LILE and HFSE enrichment: the Ángel pegmatite, central Argentina. *The Canadian Mineralogist* 52, 247-269.
- Dewaele S., Henjes-Kunst F., Melcher F., Sitnikova M., Burgess R., Gerdes A., Fernandez Alonso M., de Clercq F., Muchez P., Lehmann B. 2011. Late Neoproterozoic overprinting of the cassiterite and columbite-tantalite bearing pegmatites of the Gatumba area, Rwanda (Central Africa). *Journal of African Earth Sciences* 61, 10–26.

- Filip J., Novák M., Beran A., Zboril R. 2006. Crystal chemistry and OH defect concentrations in spodumene from different granitic pegmatites. *Physics and Chemistry of Minerals* 32, 733-746.
- Fisher D.J. 1968. Albite, variety cleavelandite, and the signs of its optic directions. *American Mineralogist* 53, 1568-1578.
- Fritschle T., Daly J.S., McConnell B., Whitehouse M.J., Menuge J.F., Buhre S., Mertz-Kraus R., Döpke D. 2018a. Peri-Gondwanan Ordovician arc magmatism in southeastern Ireland and the Isle of Man: Constraints on the timing of Caledonian deformation in Ganderia. *GSA Bulletin* 130, 1918-1939.
- Fritschle T., Daly J.S., Whitehouse M.J., McConnell B., Buhre S. 2018b. Multiple intrusive phases in the Leinster Batholith, Ireland: geochronology, isotope geochemistry and constraints on the deformation history. *Journal of the Geological Society* 175, 229-246.
- Galliski M.A., Černý P., Márquez-Zavalía M.F., Chapman R. 2012. An association of secondary Al–Li–Be–Ca–Sr phosphates in the San Elías pegmatite, San Luis, Argentina. *The Canadian Mineralogist* 50, 933-942.
- Garate-Olave I., Müller A., Roda-Robles E., Gil-Crespo P.P., Pesquera A. 2017. Extreme fractionation in a granite–pegmatite system documented by quartz chemistry: The case study of Tres Arroyos (Central Iberian Zone, Spain). *Lithos* 286-287, 162-174.
- Goldoff B., Webster J.D., Harlov D.E. 2012. Characterization of fluor-chlorapatites by electron probe microanalysis with a focus on time-dependent intensity variation of halogens. *American Mineralogist* 97, 1103-1115.
- Graham J.R., Stillman C.J. 2009. Ordovician of the south. In: Holland, C.H., Sanders, I. [eds.] *The geology of Ireland*, 2nd edition. Dunedin Academic Press, Edinburgh, Scotland, 103-117.

- Grogan S.E., Reavy R.J. 2002. Disequilibrium textures in the Leinster Granite Complex, SE Ireland: evidence for acid-acid magma mixing. *Mineralogical Magazine*, 66(6), 929-939.
- Gunn G. 2014. Critical metals handbook. American Geophysical Union, 454 p.
- Hawthorne F.C., Henry D.J. 1999. Classification of the minerals of the tourmaline group. *European Journal of Mineralogy* 11, 201–215.
- Hulsbosch N., Hertogen J., Dewaele S., Andre L., Muchez P. 2013. Petrographic and mineralogical characterisation of fractionated pegmatites culminating in the Nb-Ta-Sn pegmatites of the Gatumba area (western Rwanda). *Geologica Belgica* 16, 105-117.
- Kaeter D., Barros R., Menuge J.F., Chew D.M. 2018. The magmatic–hydrothermal transition in rare-element pegmatites from southeast Ireland: LA-ICP-MS chemical mapping of muscovite and columbite–tantalite. *Geochimica et Cosmochimica Acta* 240, 98-130.
- Kaeter D., Menuge J.F. 2017. Rare-element mineralization and metasomatism in LCT pegmatites from Leinster, SE Ireland. *Proceedings of the 8th Symposium on Granitic Pegmatites*, Kristiansand, Norway, p. 58-61.
- Kontak D. 2006. Nature and origin of an LCT-suite pegmatite with late-stage sodium enrichment, Brazil Lake, Yarmouth County, Nova Scotia. I. Geological setting and petrology. *The Canadian Mineralogist*, 44(3), 563-598.
- Kontak D.J., Kyser T.K. 2009. Nature and origin of an LCT-suite pegmatite with late-stage sodium enrichment, Brazil Lake, Yarmouth County, Nova Scotia. II. Implications of stable isotopes ($\delta^{18}\text{O}$, δD) for magma source, internal crystallization and nature of sodium metasomatism. *The Canadian Mineralogist* 47, 745-764.
- Lima A.M.C. 2000. Estrutura, mineralogia e génese dos filões aplitopegmatíticos com espodumena da Região Barroso-Alvão. PhD thesis. Universidade do Porto, 270 p.

- London D. 1987. Internal differentiation of rare-element pegmatites: effects of boron, phosphorus, and fluorine. *Geochimica et Cosmochimica Acta* 51, 403-420.
- London D. 2008. Pegmatites. *Canadian Mineralogist*, Special Publication 10, 347 p.
- London D. 2009. The origin of primary textures in granitic pegmatites. *The Canadian Mineralogist* 47, 697-724.
- London D., Morgan VI G.B. 2012. The pegmatite puzzle. *Elements*, 8, 263-268.
- Luecke W. 1981. Lithium pegmatites in the Leinster Granite (southeast Ireland). *Chemical Geology*, 34, 195-233.
- Maneta V., Baker D.R. 2014. Exploring the effect of lithium on pegmatitic textures: an experimental study. *American Mineralogist* 99, 1383-1403.
- Maneta V., Baker D.R., Minarik W. 2015. Evidence for lithium-aluminosilicate supersaturation of pegmatite-forming melts. *Contributions to Mineralogy and Petrology*, 170, 1-16.
- Manning D.A.C. 1981. The effect of fluorine on liquidus phase relationships in the system Qz-Ab-Or with excess water at 1 kb. *Contributions to Mineralogy and Petrology* 76, 206-215.
- Martin R., De Vito C. 2014. The late-stage miniflood of Ca in granitic pegmatites: an open-system acid-reflux model involving plagioclase in the exocontact. *The Canadian Mineralogist* 52, 165-181.
- McArdle P. 1984. A study of the geological setting of mineralization associated with the Tullow Lowlands Unit of the Leinster Granite. PhD thesis, 330 p.
- McArdle P., Kennan P.S. 1987. The distribution, genesis and potential of tungsten, lithium and associated metal deposits on the SE margin of the Leinster Granite. *Geological Survey of Ireland Bulletin*, 4(1), 27-40.

- McArdle P., Kennan P.S. 1992. Deformational and stratigraphic influences on mineralization in SE Ireland: *Mineralium Deposita*, v. 27, p. 213–218.
- McArdle P., Kennedy M.J. 1985. The East Carlow Deformation Zone and its regional implications. *Geological Survey of Ireland Bulletin*, 3(4), 237-255.
- Merlet C. 1994. An accurate computer correction program for quantitative electron probe microanalysis. *Microchimica Acta* 114/115, 363-376.
- Morgan VI, G.B., London D. 1987. Alteration of amphibolitic wallrocks around the Tanco rare element pegmatite, Bernic Lake, Manitoba. *American Mineralogist* 72, 1097-1121.
- O'Connor P.J., Gallagher V., Kennan P.S. 1991. Genesis of lithium pegmatites from the Leinster Granite margin, southeast Ireland: geochemical constraints. *Geological Journal* 26, 295-305.
- O'Mahony M. J. 2000. The structural and metamorphic features of the central and southern portions of the Leinster Granite Complex, SE Ireland (PhD thesis), University College Cork.
- Orville, P.M. 1963. Alkali ion exchange between vapor and feldspar phases. *American Journal of Science* 261, 201-237.
- Romeiro J.C.P., Pedrosa-Soares A.C. 2005. Controle do minério de espodumênio em pegmatitos da Mina da Cachoeira, Araçuaí, Brasil. *Geonomos* 13, 75-81.
- Shearer C.K., Papike J.J., Joliff B.L. 1992. Petrogenetic links among granites and pegmatites in the Harney Peak rare-element granite-pegmatite system, Black Hills, South Dakota. *Canadian Mineralogist* 30, 785-809.
- Shearer C.K., Papike J.J., Simon S.B., Laul J.C. 1986. Pegmatite-wallrock interactions, Black Hills, South Dakota: Interaction between pegmatite-derived fluids and quartz-mica schist wallrock. *American Mineralogist* 71, 518-539.

- Steiger R., Von Knorring O. 1974. A lithium pegmatite belt in Ireland. *Journal of Earth Sciences, Leeds Geological Association*, 8, 433-443.
- Stock M.J., Humphreys M.C., Smith V.C., Johnson R.D., Pyle D.M., EIMF. 2015. New constraints on electron-beam induced halogen migration in apatite. *American Mineralogist* 100, 281-293.
- Stormer J., Pierson M.L., Tacker R.C. 1993. Variation of F and Cl X-ray intensity due to anisotropic diffusion in apatite. *American Mineralogist* 78, 641-648.
- Swanson S.E. 2012. Mineralogy of spodumene pegmatites and related rocks in the tin–spodumene belt of North Carolina and South Carolina, USA. *The Canadian Mineralogist* 50, 1589-1608.
- Sweetman T.M. 1988. The geology of the Blackstairs Unit of the Leinster Granite. *Irish Journal of Earth Sciences*, 9(1), 39-59.
- Thomas R., Davidson P. 2016. Revisiting complete miscibility between silicate melts and hydrous fluids, and the extreme enrichment of some elements in the supercritical state — Consequences for the formation of pegmatites and ore deposits: *Ore Geology Reviews* 72, 1088–1101.
- Tietzsch-Tyler D., Sleeman A.G. 1994. Geology of Carlow-Wexford: a geological description to accompany the bedrock geology 1:100,000 map series, sheet 19, Carlow-Wexford. Geological Survey of Ireland, 57 p.
- Tischendorf G., Förster H.-J., Gottesmann B., Rieder M., 2007. True and brittle micas: composition and solid-solution series. *Mineralogical Magazine* 71, 285-320.
- USGS - United States Geological Survey. 2018. Mineral commodity summaries 2018, 200 p.
- USGS - United States Geological Survey. 2019. Mineral commodity summaries 2019, 200 p.
- Whitney D.L., Evans B.W. 2010. Abbreviations for names of rock-forming minerals. *American Mineralogist* 95, 185-187.

- Whitworth M.P. 1992. Petrogenetic implications of garnets associated with lithium pegmatites from SE Ireland. *Mineralogical Magazine* 56, 75-83.
- Whitworth M.P., Rankin A.H. 1989. Evolution of fluid phases associated with lithium pegmatites from SE Ireland. *Mineralogical Magazine* 53, 271-284.
- Wise M.A., Brown C.D. 2010. Chemical composition of coexisting columbite-group minerals and cassiterite from the Black Mountain pegmatite, Maine. *European Journal of Mineralogy* 23, 817–828.
- Wood S.A., Williams-Jones A.E. 1993. Theoretical studies of the alteration of spodumene, petalite, eucryptite and pollucite in granitic pegmatites: exchange reactions with alkali feldspars. *Contributions to Mineralogy and Petrology* 114, 255-263.

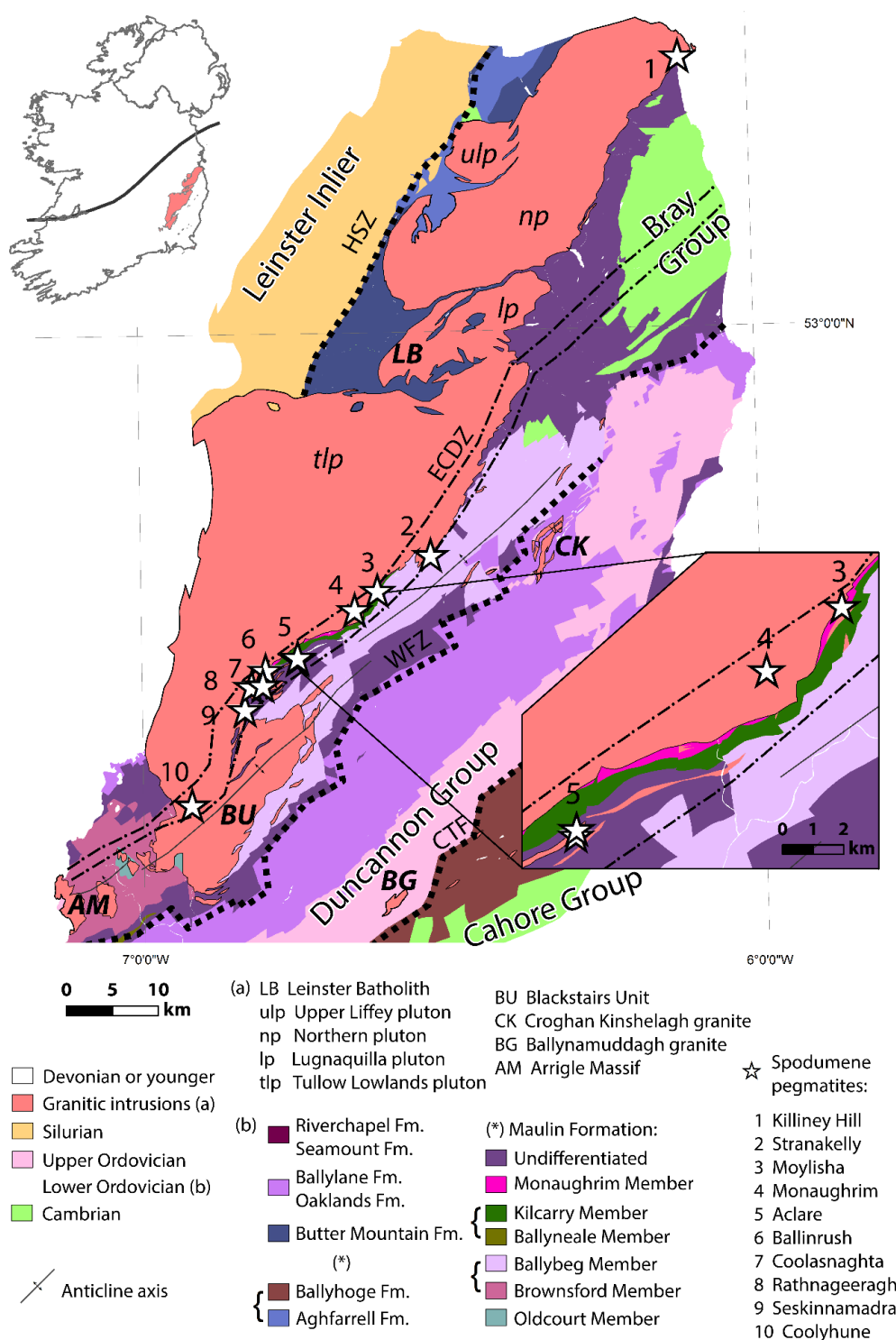


Figure 1. Granitic intrusions (in bold capital letters, and lower case letters for plutons within the Leinster Batholith) and spodumene pegmatites (numbered stars) along with detailed stratigraphy of country rocks of the Ribband Group in Leinster. Inset shows detail of localities described in the text. Major structures from the west: HSZ = Hollywood Shear Zone, ECDZ = East Carlow Deformation Zone (from McArdle and Kennedy 1985); WFZ = Wicklow Fault Zone (from McConnell et al. 1999); CTF = Courtown-Tramore Fault (from Graham and Stillman 2009). Geological units from the 1:500000 geological mapping shapefiles of the Geological Survey Ireland. Curly brackets represent laterally equivalent units. Anticlines from Tietzsch-Tyler and Sleeman (1994).

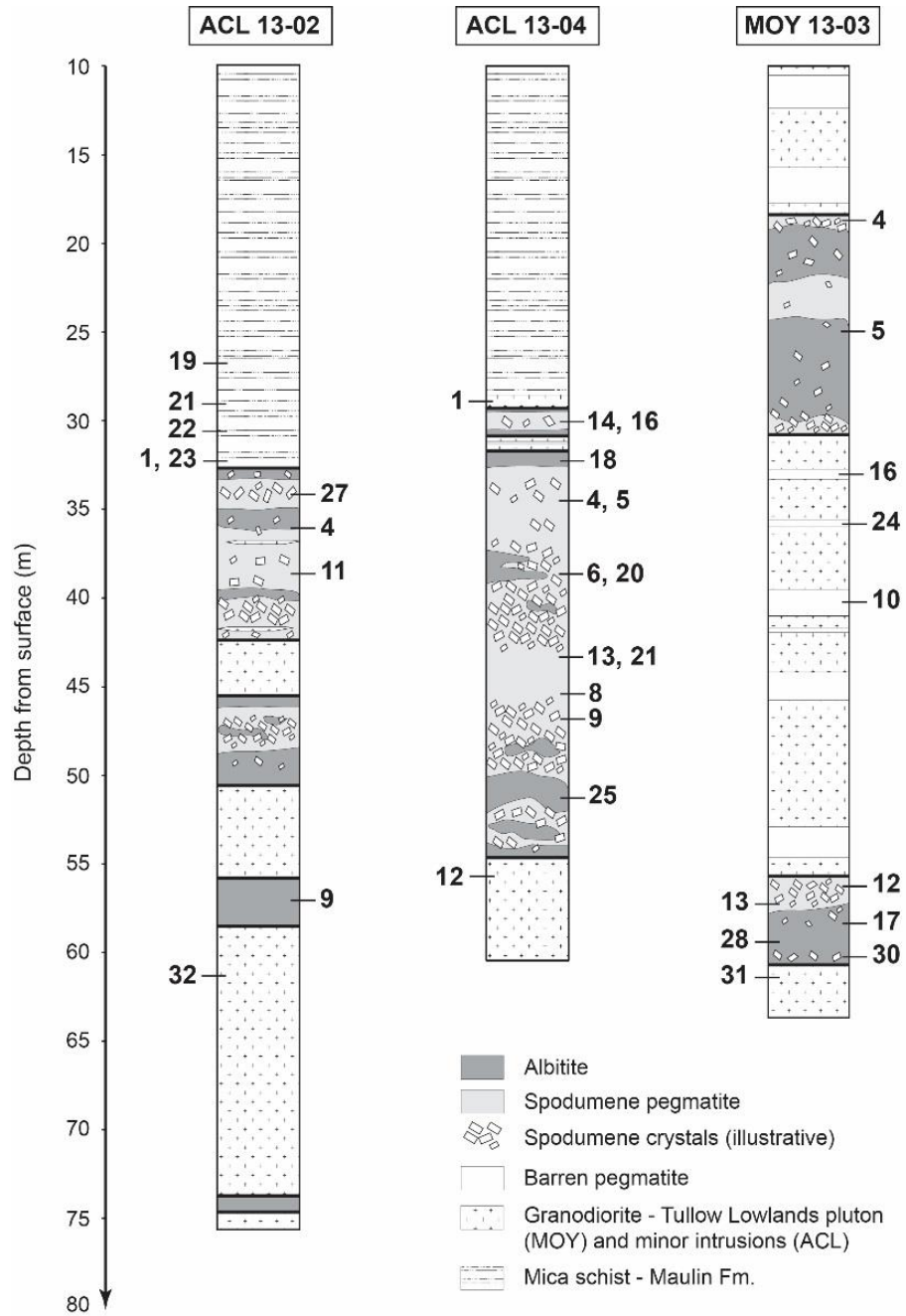


Figure 2. Simplified geology of drill cores and location of samples (numbers) studied. Drill core ACL 13-04 represents the zoned pegmatite intersection.

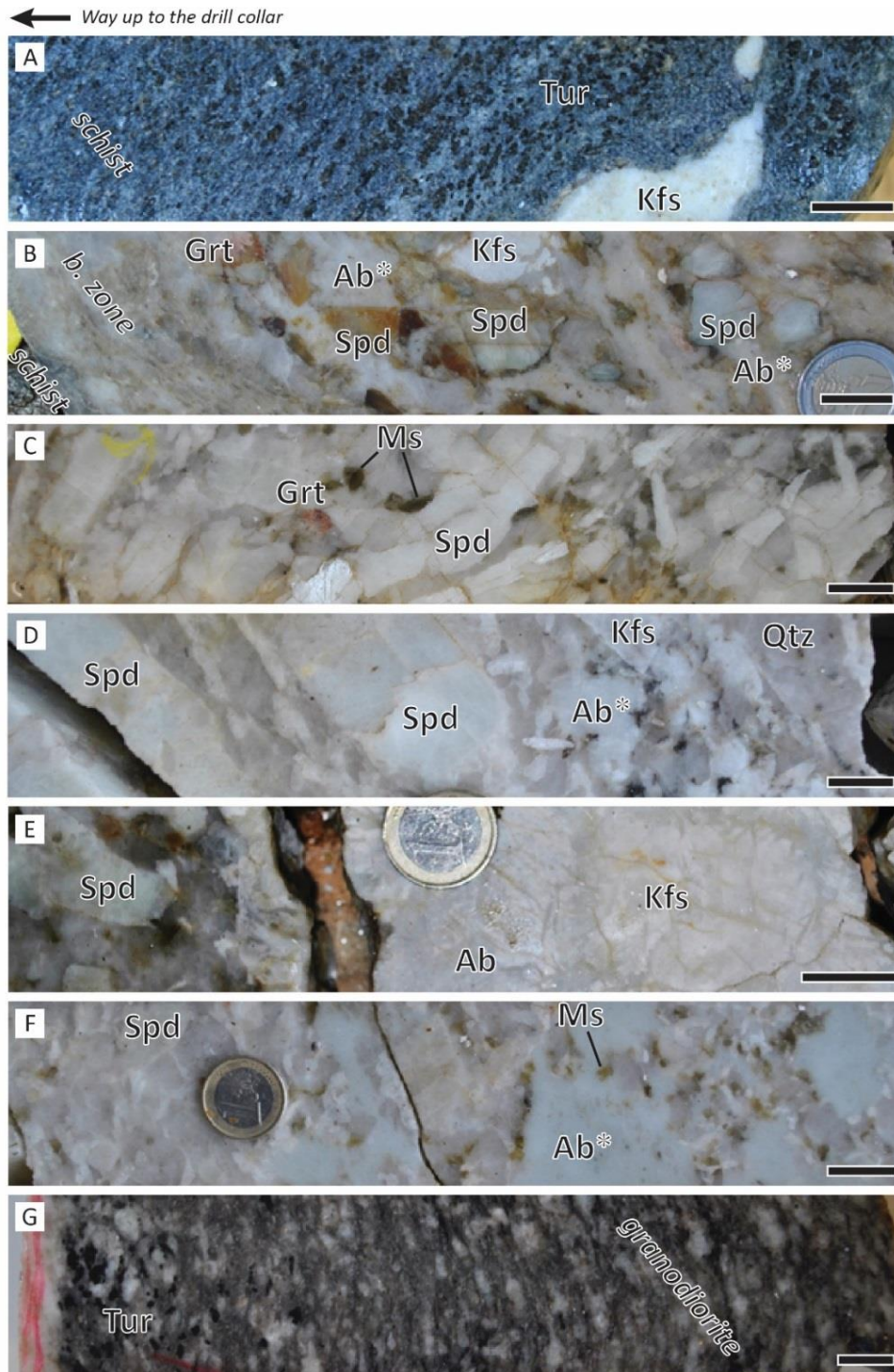


Figure 3. Pegmatite intersections and wallrocks drilled in Aclare. Mineral abbreviations: Ab* = albitite (fine-grained, often replacive), others as in Whitney and Evans (2010). Scale bar represents 2 cm. (A) Tourmalinised mica schist adjacent to spodumene pegmatite, with a pegmatitic quartz-feldspathic boudin. (B) Relatively fine-grained and foliated border zone with quartz, feldspar and mica, followed by spodumene, K-feldspar and garnet megacryst relics within albitite; note alteration (dark green) common in borders of spodumene crystals. (C) Typical unaltered primary pegmatite assemblage of spodumene, quartz, muscovite and garnet; note pearly luster of spodumene and deformation and fracturing of elongate crystals. (D) Coarse-grained, fractured spodumene and medium-grained spodumene adjacent to quartz and albitite. (E) Abrupt change from spodumene, quartz and green muscovite zone (left) to massive K-feldspar, with minor radiating albite, in the core zone. (F) Interstitial light blue albitite containing abundant fine-grained apatite, within spodumene, feldspars, quartz and muscovite. (G) Tourmaline in footwall foliated granodiorite adjacent to spodumene pegmatite. A-C: ACL 13-02; D-G: ACL 13-04.

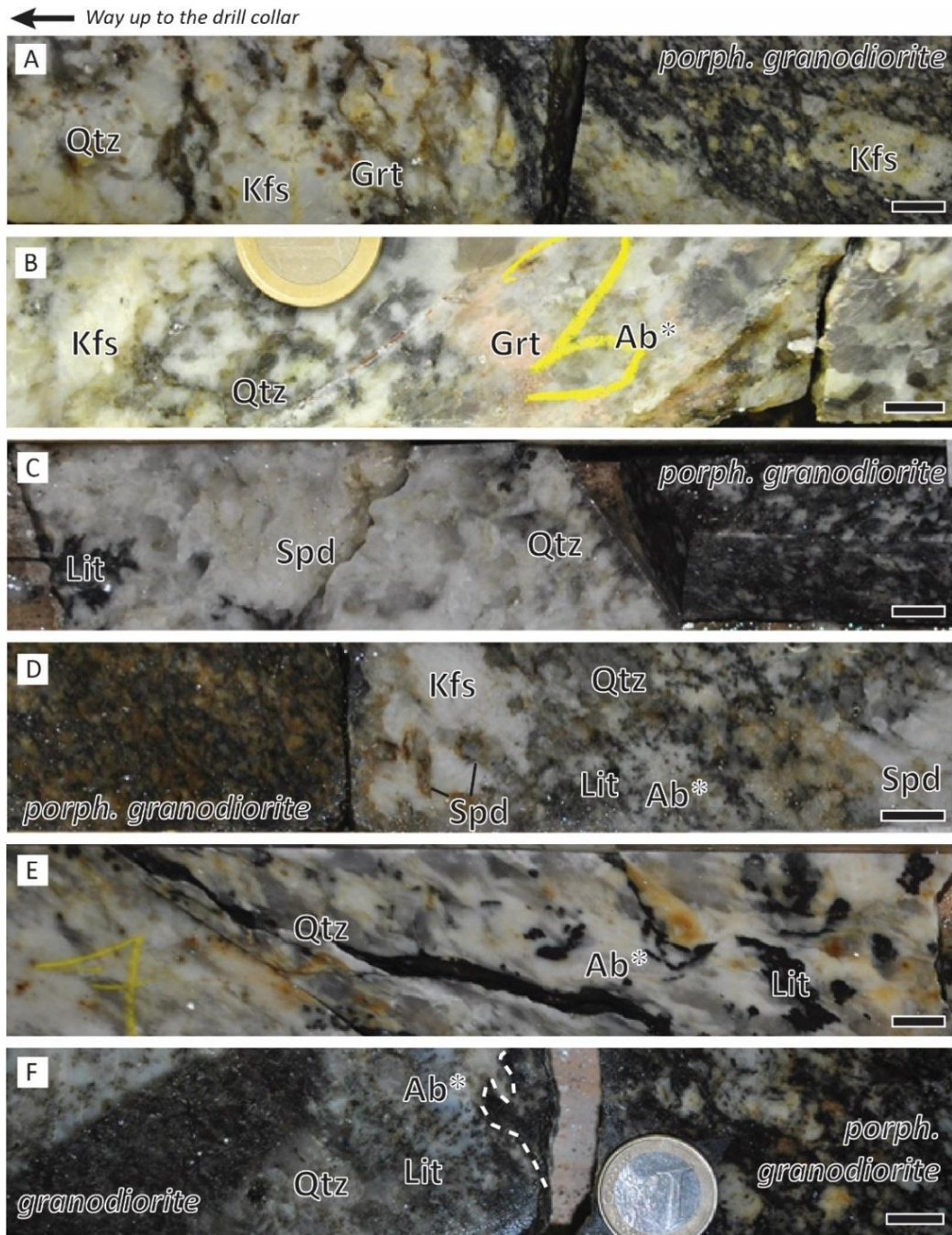


Figure 4. Pegmatite intersections and wallrocks in Moylisha drill core MOY 13-03. Mineral abbreviations: Ab* = albitite (fine-grained, often replacive), Lit = lithiophilite, others as in Whitney and Evans (2010). Scale bar represents 1 cm. (A) Sheared barren pegmatite in contact with locally foliated porphyritic granodiorite. (B) Barren pegmatite and replacive albitite, with fine-grained light pink garnet clusters. (C) Abrupt and irregular lower contact of spodumene pegmatite, dominated by spodumene, K-feldspar and quartz, with foliated granodiorite. (D) Upper contact of spodumene pegmatite, dominated by partially altered spodumene (light green) and K-feldspar, as well as albitite with lithiophilite, in contact with foliated granodiorite. (E) Fracture filling lithiophilite within albitite, with crystal elongation parallel to the fabric. (F) Irregular lower contact of spodumene pegmatite with granodiorite (surface indicated with dashed line), with altered granodiorite xenolith on the left.

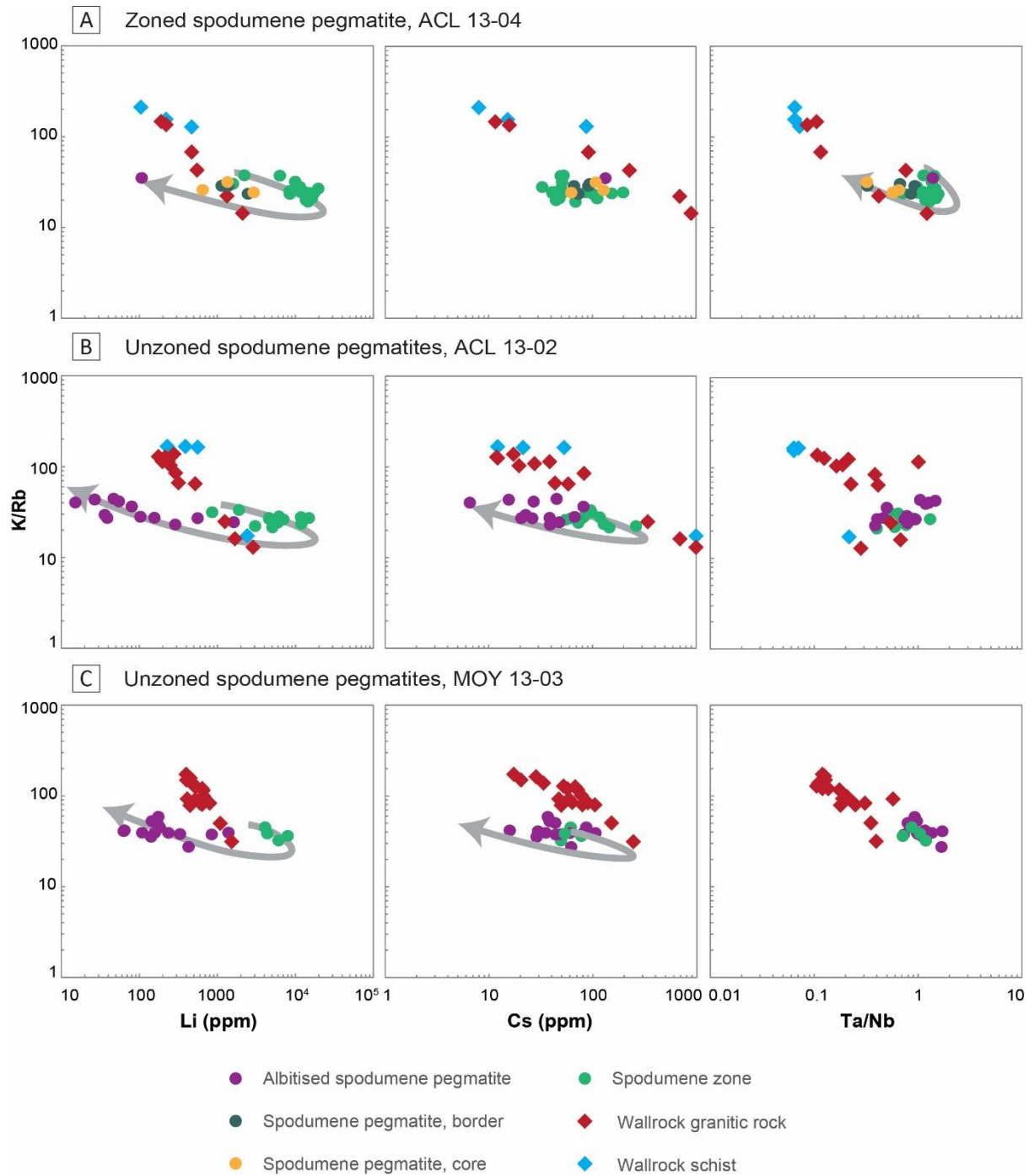


Figure 5. Geochemical variation (K/Rb versus Li, Cs and Ta/Nb) observed in whole-rock compositions of the three drill cores studied. **(A)** Zoned Aclare spodumene pegmatite and wallrocks. **(B)** Unzoned Aclare spodumene pegmatites and wallrocks. **(C)** Moylisha unzoned pegmatites and wallrocks. Grey arrows indicate identifiable internal geochemical evolution trends of pegmatites.

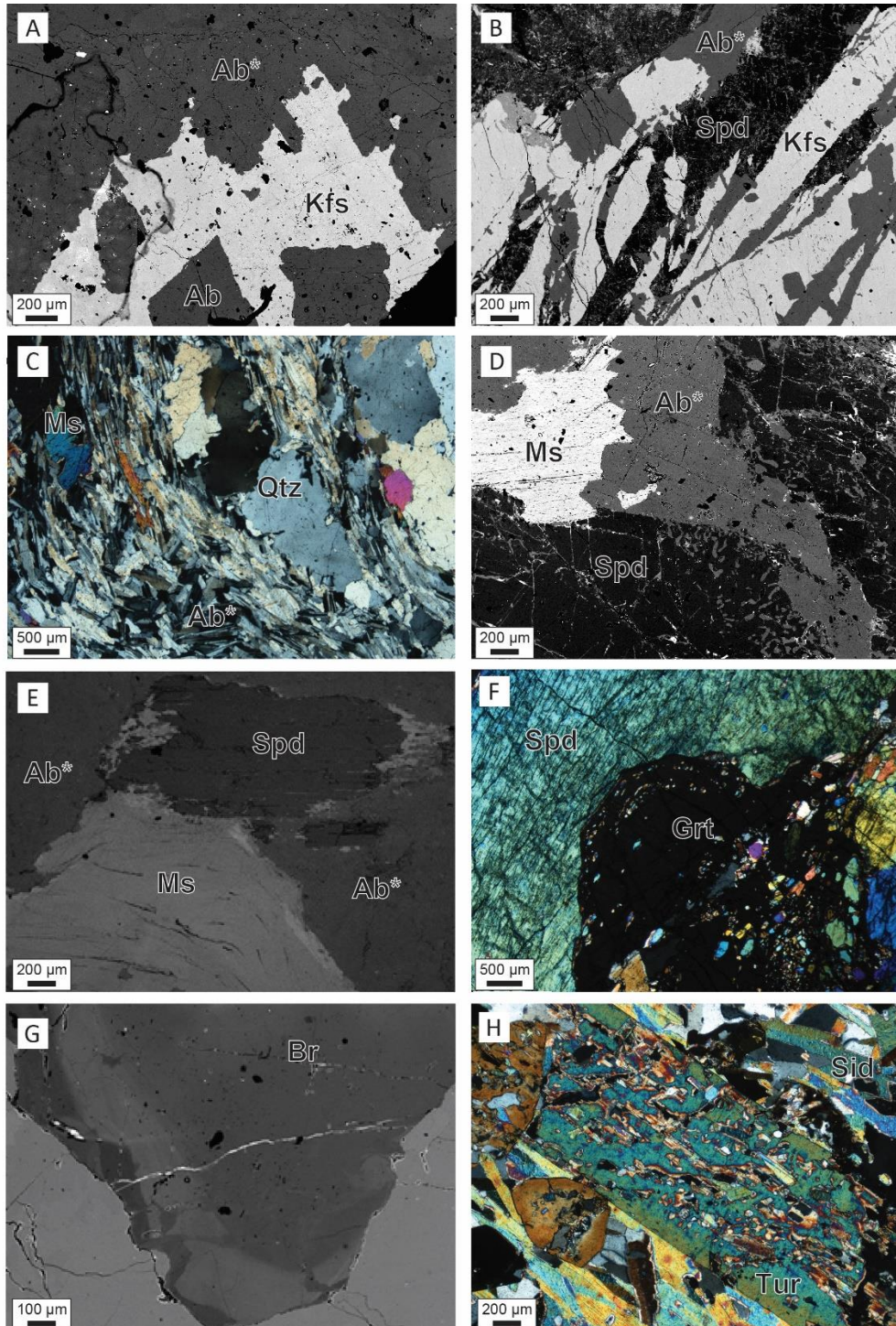


Figure 6. Microscopic features in pegmatites and wallrock. Mineral abbreviations: Ab* = albitite (fine-grained, often replacive), others as in Whitney and Evans (2010). (A) Possibly magmatic intergrowth of K-feldspar and tabular albite overgrown by replacive albite in spodumene pegmatite, sample MOY 13-03/4. (B) Saccharoidal albite in veinlets crosscutting K-feldspar and spodumene, ACL 13-04/5. (C) Late albitite wrapping early primary minerals, sample ACL 13-04/16. (D) Spodumene and muscovite within fine-grained replacive albite, note symplectic spodumene-albite intergrowths at the bottom, sample ACL 13-02/2. (E) Early primary muscovite with lighter grey borders of polyolithionite after alteration of spodumene, sample MOY 13-03/4. (F) Garnet and spodumene intergrowth, sample ACL 13-04/20. (G) Early primary coarse-grained beryl in the zoned pegmatite, spodumene zone, with irregular zonation pattern and Cs enrichment in bright portions, sample ACL 13-04/9. (H) Medium-grained zoned tourmaline crystals within siderophyllite in spodumene pegmatite exocontact in mica schist, sample ACL 13-02/1. C, F and H are crossed polarized transmitted light images; other images SEM BSE.

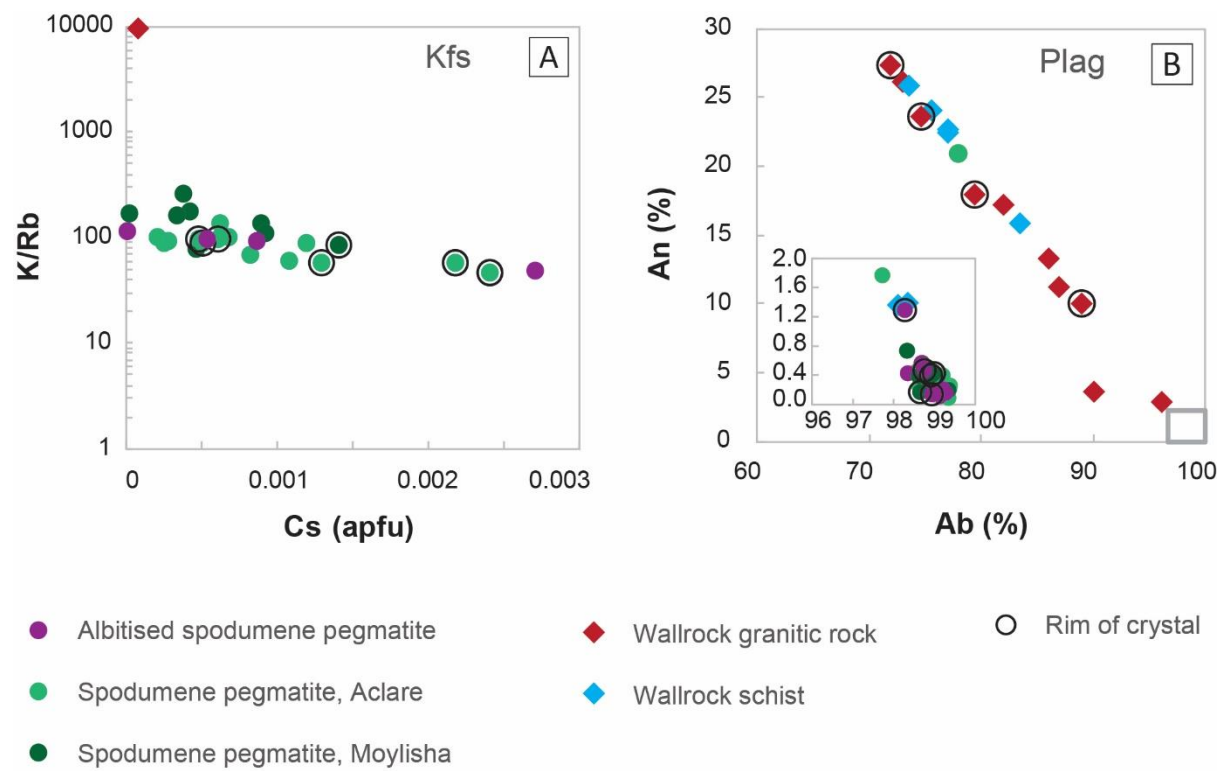


Figure 7. Chemistry of feldspars in pegmatites and wallrocks. **(A)** K/Rb versus Cs in K-feldspar. **(B)** Anorthite and albite molecule in plagioclase.

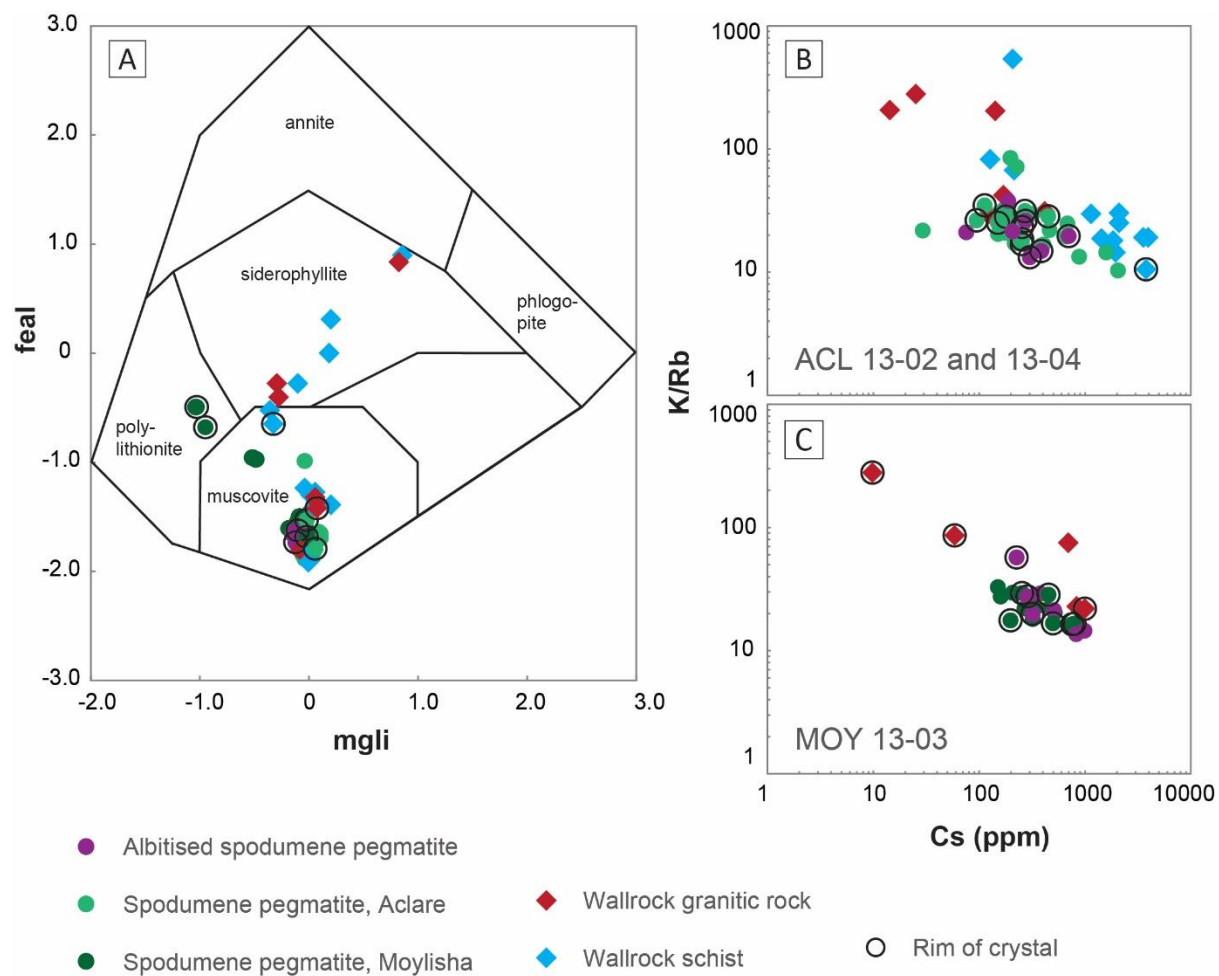


Figure 8. Chemistry of micas in pegmatites and wallrocks. (A) Composition in the $mgli$ versus $feal$ diagram (Tischendorf et al. 2007). (B) and (C) K/Rb against Cs (ppm) for muscovite in ACL13-02,-4 and MOY13-3, respectively.

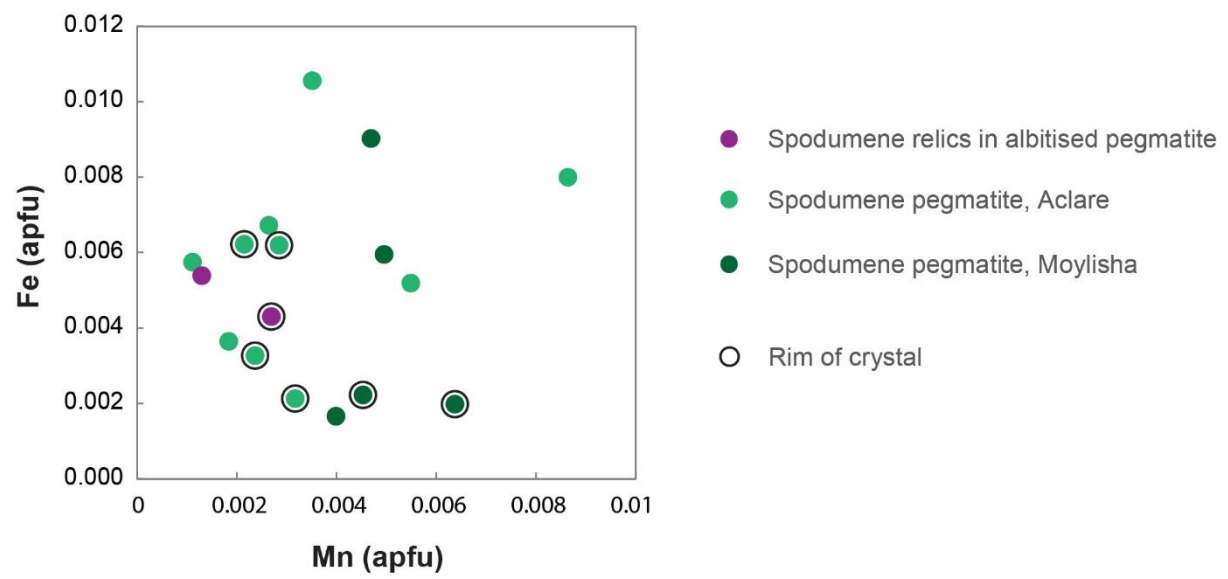


Figure 9. Mn and Fe (apfu) variation in spodumene.

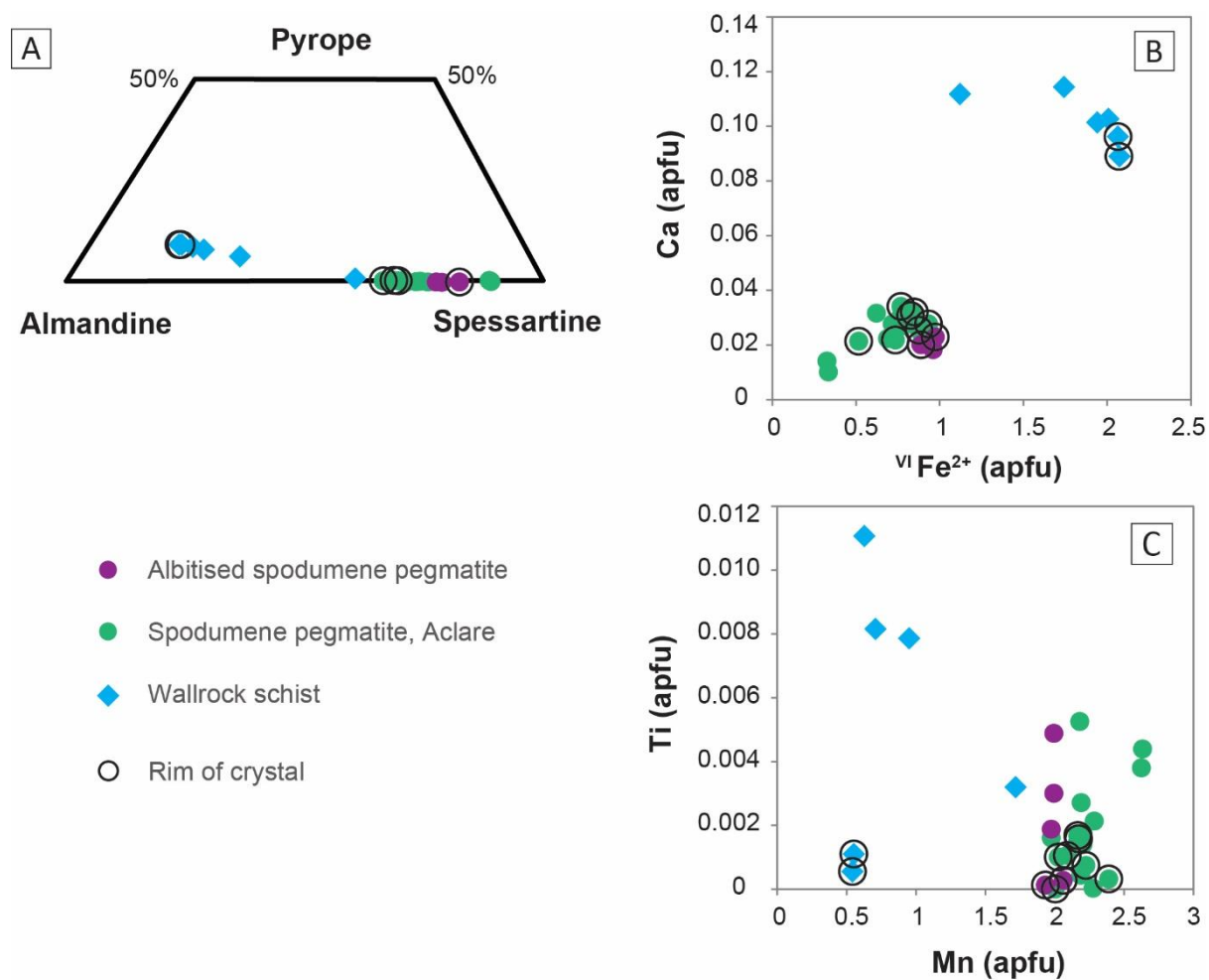


Figure 10. Variation plots of garnet. **(A)** Triangular plot almandine-spessartine-pyrope. **(B)** Variation plot of Fe^{2+} against Ca. **(C)** Variation plot of Mn against Ti (apfu), displaying contrasting compositions of garnet in schist and spodumene pegmatites.

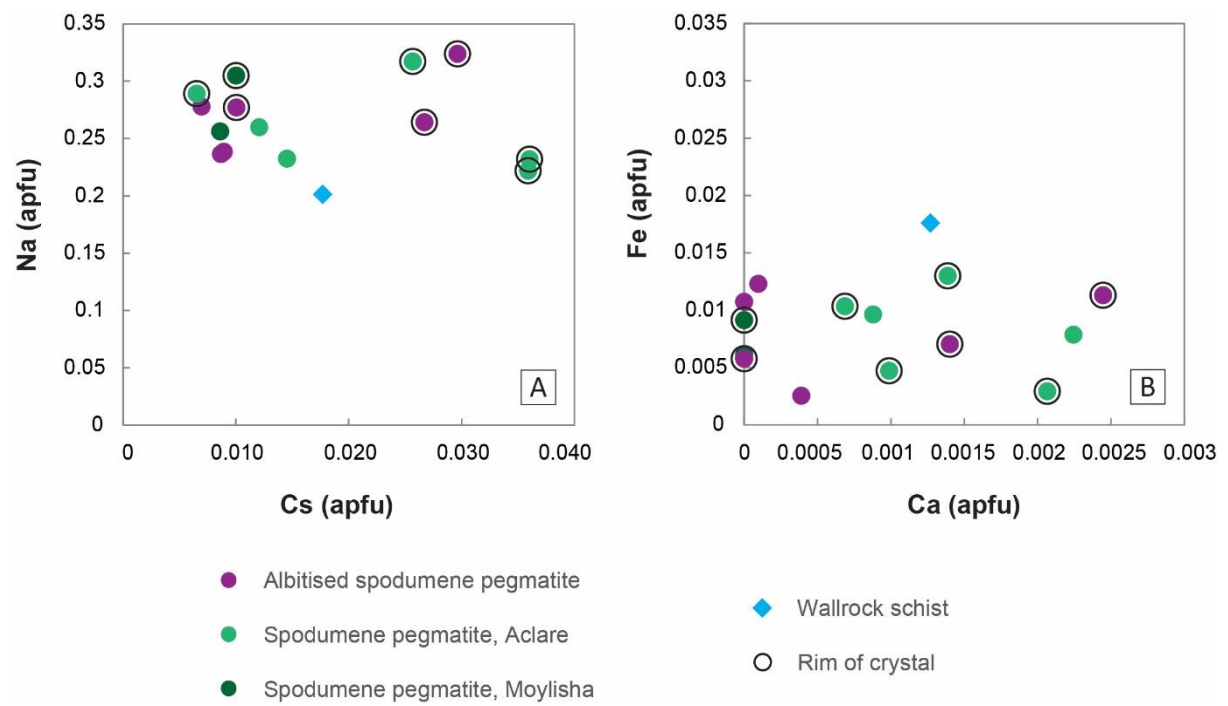


Figure 11. Variation plots of beryl. (A) Cs against Na (apfu) and (B) Ca against Fe (apfu).

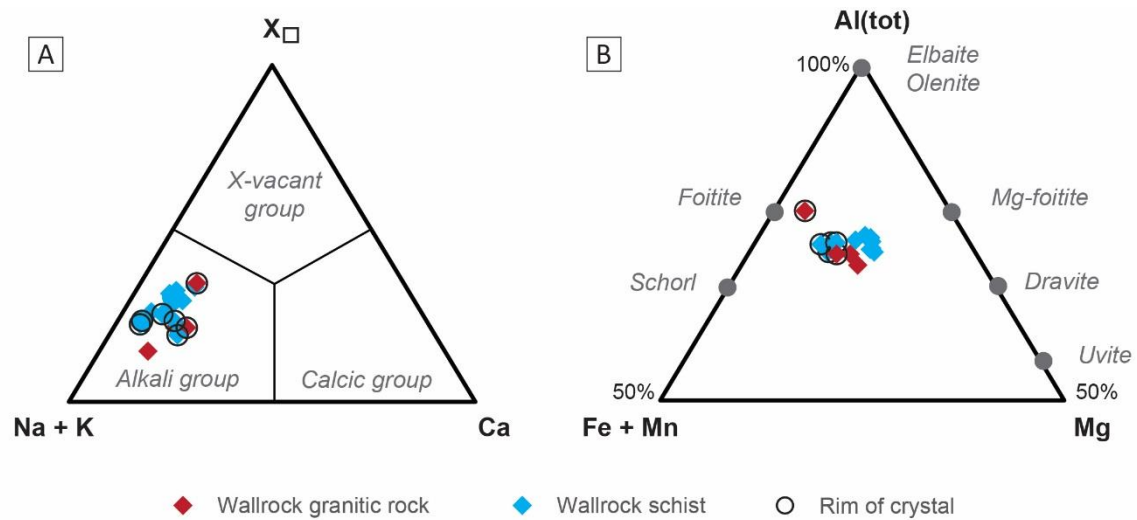


Figure 12. Compositional variation of tourmaline after diagrams of Hawthorne and Henry (1999). **(A)** Triangular plot X_{\square} -Na + K-Ca. **(B)** Triangular plot $Al(tot)$ -Fe + Mn-Mg.

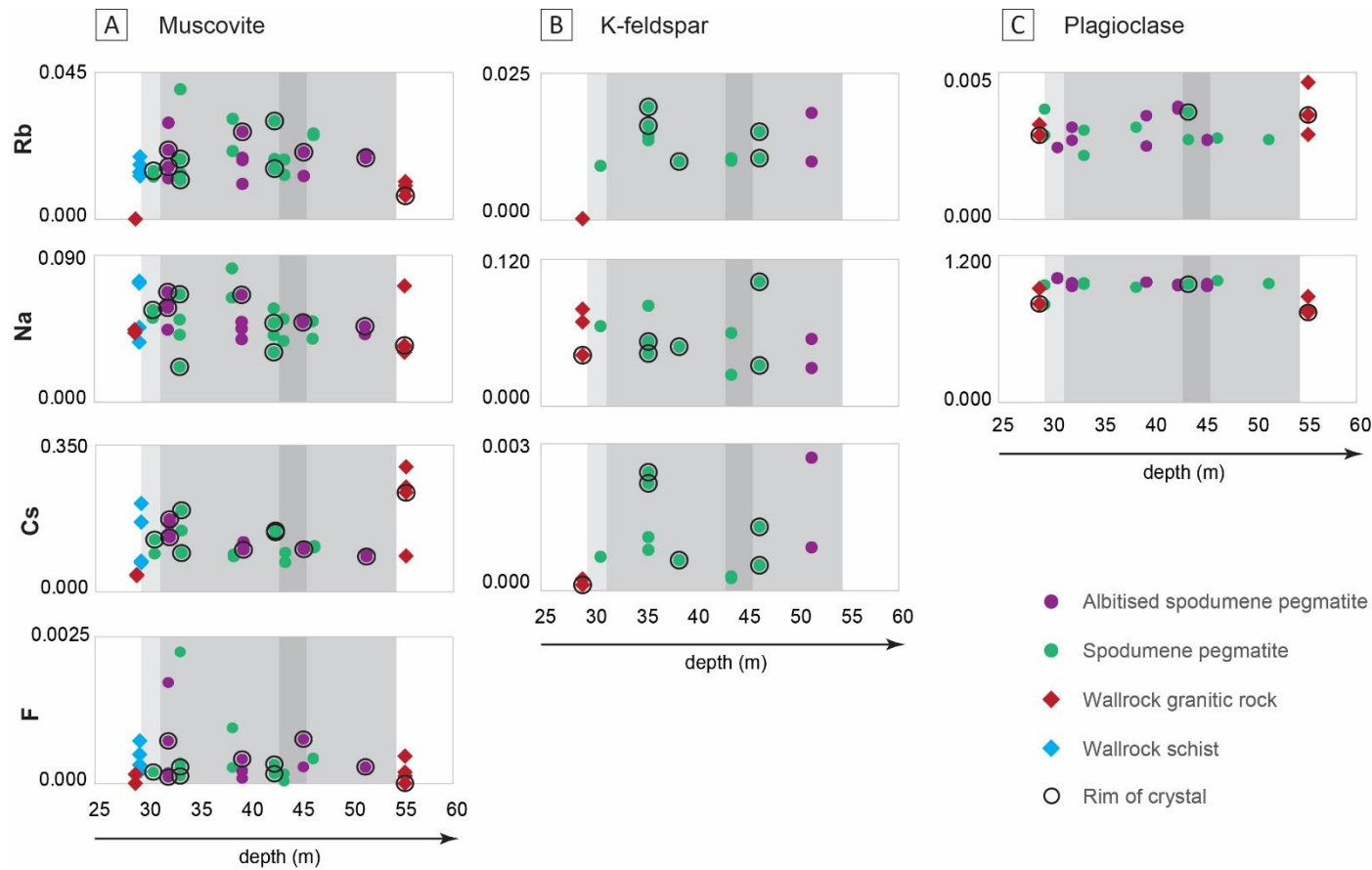


Figure 13. Compositional variation of main early primary minerals and relationship with zonation in intersection ACL 13-04. (A) and (D) Spodumene.

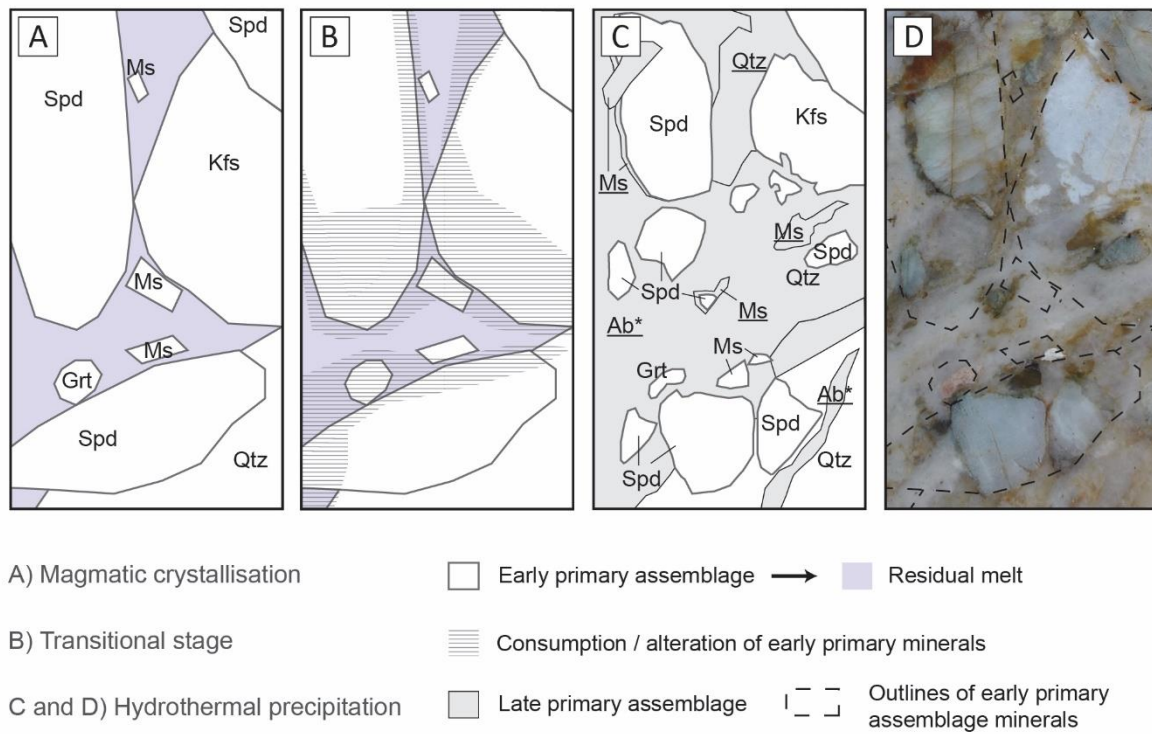


Figure 14. Schematic internal evolution of Leinster pegmatites based on the magmatic-hydrothermal model of Kaeter et al. (2018). **(A)** Stage 1: early primary assemblage (magmatic crystallisation phase) and residual melt. **(B)** Stage 2: consumption of early primary minerals in the transitional magmatic-hydrothermal stage. **(C)** Stage 3: crystallisation of residual liquid after consumption of early primary minerals, resulting in the late primary assemblage (minerals underlined). Note rims of hydrothermal muscovite around early primary minerals. **(D)** Core sample sketched in C compared with possible extent of early primary minerals before consumption (dashed lines).

Table 1. Summary of mineralogy and textures of spodumene pegmatites and country rocks in the drill cores studied.

	ACL 13-02	ACL 13-04	MOY 13-03
<i>Spodumene pegmatites</i>			
Border	Up to 3cm thick, alternating Ab-rich and Ms-rich bands; 0.5-1.0 mm Ab (20-40%), Ms (20-40%), Qz (20-40%), Grt (1%) ± Kfs, Brl; comb Ms and rarely Spd		Up to 1cm thick, a 0.5-1.0 mm Ab (20-40%), Ms (20-40%), Qz (20-40%), Grt (1%) ± Kfs, Brl
Spodumene intervals	Millimetre to 7 cm scale Spd (10-30%, subhedral short to elongate prisms or laths), Qz (20-30% anhedral, interstitial), Kfs (10-30%, often perthitic), Ab (5-10%, tabular), Ms (5-10% subhedral flakes) ± Grt (subhedral to euhedral with Qz and Pl inclusions, often intergrown with Spd and Ap), Brl (subhedral prisms), F-rich Ap (anhedral), Cst, Sp; deepest intervals fully albitised	Millimetre to 10 cm scale Spd (10-35%, subhedral short to elongate prisms or laths), Qz (20-30% anhedral, interstitial), Kfs (10-30%, often perthitic and inclusion-rich), Ab (5-10%, tabular), Ms (5-10% subhedral flakes) ± Grt (subhedral to euhedral with Qz and Pl inclusions, often intergrown with Spd and Ap), Brl (subhedral prisms), F-rich Ap (anhedral), Cst, Sp	Millimetre to 2 cm scale Spd (10-35%, subhedral short to elongate prisms or laths), Qz (20-30% anhedral, interstitial), Kfs (10-30%, often perthitic and inclusion-rich), Ab (5-10%, tabular), Ms (5-10% subhedral flakes) ± Grt (subhedral to euhedral with Qz and Pl inclusions, often intergrown with Spd and Ap), Brl (subhedral prisms), F-rich Ap (anhedral), Cst, Sp
Core zone	None	Coarse-grained Kfs-Ms-Qz-Pl, with Pl often as radiating crystals in the thickest intersection.	None
Albitite	Saccharoidal, mm or smaller scale crystals, replacement / interstitial patches within spodumene and core zones, 0-15% of rock volume; Ab and strained Qz sometimes elongated subparallel to pegmatite contacts and wallrock foliation, composed of Ab (>90%), Qz, Ms, F-rich Ap, Brl, Cst, Sp, Pol, Zrn, Py, CCp, Apy, Urn, Lith, CGMs.		Saccharoidal, mm or smaller scale crystals, replacement / interstitial patches within spodumene and core zones, 0-15% of rock volume; Ab and strained Qz sometimes elongated subparallel to pegmatite contacts and wallrock foliation, composed of Ab (>90%), Qz, Ms, F-rich Ap, Brl, Cst, Sp, Pol, Zrn, Py, CCp, Apy, Urn, Lith, CGMs.
<i>Country rocks</i>			
Hangingwall	Fine-grained schist, Ms (30%), Chl (35%), Bt (5%), Qz (15%), Pl (5%), Kfs (5%), Py (3%) ± Zrn, Ccp, Rt; strong mica-parallel metamorphic foliation, sometimes crenulated, including occasional 1-10 cm thick Qz-Fsp bands; 0.5-3 mm porphyroblasts: Grt foliation-elongate and St, And overgrowing or wrapped around by foliation	Granodiorite, 0.5-3 mm inequigranular, Qz (35-40%), Ogc (25-30%), Mc (15-20%, subhedral blocky), Bt (10-15%, often chloritized), Ms (5%) and accessory Ap, Zrn, Mag, Py; strong metamorphic foliation defined by micas and elongated quartz, sometimes including relict Ogc phenocrysts (~1 cm, subhedral tabular, zoned with sericitized cores)	Granodiorite, sparitic, with inclusions of Ogc, (35%), Ogc (35%) and accessory Chl, Bt, and foliation defined by micas and elongated quartz
Footwall	Granodiorite, 0.5-3 mm inequigranular, Qz (35-40%), Ogc (25-30%), Mc (15-20%, subhedral blocky), Bt (10-15%, often chloritized), Ms (5%) and accessory Ap, Zrn, Mag, Py; strong metamorphic foliation defined by micas and elongated Qz, sometimes including relict Ogc phenocrysts (~1 cm, subhedral tabular, zoned with sericitized cores)		Granodiorite 1-3 cm scale, (15-30%), Bi (5-10%), and foliation defined by micas and elongated quartz

